ANL/KP-21/1
KP-RPT-000139

Thermochemical Modeling in Molten Fluoride Salts for Radionuclide Speciation

Nuclear Science and Engineering Division,
Argonne National Laboratory

Kairos Power

About Argonne National Laboratory

Argonne is a U.S. Department of Energy laboratory managed by UChicago Argonne, LLC under contract DE-AC02-06CH11357. The Laboratory's main facility is outside Chicago, at 9700 South Cass Avenue, Argonne, Illinois 60439. For information about Argonne and its pioneering science and technology programs, see www.anl.gov.

ANL/KP-21/1
KP-RPT-000139

Thermochemical Modeling in Molten Fluoride Salts for Radionuclide Speciation

Prepared by
Shayan Shahbazi, Matthew Bucknor
Nuclear Science and Engineering Division, Argonne National Laboratory

Sara Thomas
Chemical and Fuel Cycle Technologies Division, Argonne National Laboratory

Augustus Merwin, Quan Zhou
Kairos Power

February 2021

Acknowledgements

This report is part of a collaboration between Argonne National Laboratory and Kairos Power to support research in mechanistic source term and safety analysis of Kairos Power's fluoride salt-cooled high-temperature reactor (KP-FHR). This material is based upon work supported by the U.S. Department of Energy, Office of Nuclear Energy, under Award Number DE-NE-0008854. The authors would like to thank Ted Besmann and Jake McMurray for reviewing this report.

Executive Summary

An important aspect of the licensing process for nuclear reactors is providing a reasonable assurance of safety to the general public. This includes modeling potential radionuclide releases from the reactor during normal operations and accident scenarios, which is known as the reactor's source term. A new class of advanced (non-LWR) reactors are being developed which use molten salts as the coolant fluid. Because the molten salt coolant represents a credited barrier for radionuclide transport between the fuel and the environment, a necessary aspect of mechanistic source term (MST) analysis for the KP-FHR is modeling the thermochemistry of molten salts. Provided here is a review of the theory of the thermodynamic principles governing multicomponent phase equilibria, the background of molten salt thermochemistry research, and a summary of the thermochemical data relevant to the KP-FHR coolant salt, Li_2BeF_4, commonly referred to as "FLiBe". A review of literature is followed by a brief introduction to methods that can be used to model the thermochemical behavior of molten salt mixtures. The methodology outlined is based on the use of a commercial thermodynamic modeling software called FactSage, which is one of only a few available softwares based on the modified quasichemical model (MQM), which is the recommended solution model for molten salts.

Table of Contents

Acronyms

Acronym	Definition
ANL	Argonne National Laboratory
ANPP	Aircraft Nuclear Propulsion Program at ORNL
CALPHAD	Calculation of Phase Diagrams approach
CCT	coordination cluster theory of solutions
CIS	conformal ionic solution theory of solutions
DOE-NE	U.S. Department of Energy, Office of Nuclear Energy
FHR	fluoride salt-cooled high temperature reactor
FLiBe	Li_2BeF_4
FNN	first-nearest-neighbor
JRC	European Commission's Joint Research Centre
KP	Kairos Power
LWR	light water reactor
MQM	modified quasichemical model of solutions
MSBR	Molten Salt Breeder Reactor
MSDR	Molten Salt Demonstration Reactor
MSR	molten salt reactor
MSRE	Molten Salt Reactor Experiment
MSRP	Molten Salt Reactor Program at ORNL
MST	mechanistic source term
MSTDB-TC	Molten Salt Thermodynamic Database – Thermochemical Properties
NEAMS	Nuclear Energy Advanced Modeling and Simulation program
NRC	Nuclear Regulatory Commission
ORNL	Oak Ridge National Laboratory
QCT	quasichemical theory of solutions
QKTO	one-lattice polynomial model in FactSage
SNN	second-nearest-neighbor
SRO	short range ordering
SUBQ	two-lattice modified quasichemical model (revised) in FactSage
TRISO	tri-structural isotropic fuel
TSLM	two-sublattice ionic liquid model
TSQA	two sublattice quadruplet approximation

1 Introduction

An important aspect of the licensing process for nuclear reactors is providing a reasonable assurance of safety to the general public. This includes modeling potential radionuclide releases from the reactor during normal operations and accident scenarios, which is known as the reactor's source term. While source terms were historically found using conservative, bounding assumptions based on experimental data, there has been an emphasis in the last quarter century on modeling the reactor's source term with more physics-based modeling and more realistic phenomena. This mechanistic approach to source term analysis includes consideration and/or modeling of all layers of protection between the radionuclides and the environment.

A new class of advanced (non-LWR) reactors are being developed which use molten salts as the coolant fluid. Kairos Power is developing one such reactor known as the fluoride salt-cooled high temperature reactor (KP-FHR), which uses molten fluoride salt as a coolant for fuel matrix pebbles packed with TRISO fuel particles. Because the molten salt coolant represents a credited barrier for radionuclide transport between the fuel and the environment, a necessary aspect of mechanistic source term (MST) analysis for the KP-FHR is modeling the thermochemistry of molten salts.

Provided here is a review of the theory of the thermodynamic principles governing multicomponent phase equilibria, the background of molten salt thermochemistry research, and a summary of the thermochemical data relevant to the KP-FHR coolant salt, Li_2BeF_4, commonly referred to as "FLiBe". Especially important is the research which took place over nearly three decades at Oak Ridge National Laboratory (ORNL) starting around 1950, during which there were two successive multidisciplinary efforts to construct molten salt reactors, starting with the Aircraft Nuclear Propulsion Program (ANPP), and followed by the Molten Salt Reactor Program (MSRP). Molten salt thermochemistry research would continue at many institutions with the development of molten salt solution models, which better approximate the behavior of the components in molten salt mixtures compared to those models developed for other types of liquid solutions.

A review of literature is followed by a brief introduction to methods that can be used to model the thermochemical behavior of molten salt mixtures. While chemical and phase equilibria can often be modeled simply with Gibbs free energy minimization methods based on thermodynamic quantities for the pure components, molten salts are not thermodynamically ideal. This results in the additional step of having to measure or estimate activity coefficient data for components in the mixture which experience deviations from ideality. While activity coefficients are typically measured experimentally, such experiments have not been carried out for many different components in various molten salt mixtures. It is therefore desirable to use the aforementioned liquid solution models, which approximate molten salt solutions well, in modeling the mixture thermodynamics which can be used to estimate activity coefficient data.

The methodology outlined is based on the use of a commercial thermodynamic modeling software called FactSage, which is one of only a few available softwares based on the modified quasichemical model (MQM). As will be discussed, MQM is the recommended solution model which utilizes thermodynamic data from pseudobinary systems (mixtures of two compounds)

to approximate the thermodynamics of higher order and multicomponent mixtures. Additionally, FactSage can use Gibbs minimization to complete speciation calculations and provide phase equilibria data for the system. This data can then be used to calculate theoretical activity coefficients for each component based on knowledge of the pure component vapor pressures. Activity coefficient data is necessary to accurately model the vaporization of radionuclides from a molten salt coolant, which rarely behaves in an ideal manner, and ultimately this information is necessary to analyze the source term mechanistically.

For systems where activity coefficient data is unavailable, bounding estimates of activity coefficients can be made based on trends from analogous systems where data is available. Such approximations are expected to be utilized in mechanistic source terms where analyses will need to span a variety of melt compositions. This review summarizes the relevant trends in solute chemistry and is intended to facilitate the most accurate assessments of such systems as much as possible. It is noted that the majority of available experimental data and relevant information has historically focused on liquid-fueled reactors in which solute species of interest are present at concentrations that are significant fractions of their solubility limits. The KP-FHR differs fundamentally from such reactor designs in this respect as solute concentrations will be limited to dilute levels. For source term analyses of the KP-FHR, it is emphasized that the solutions of interest will be nearly pure FLiBe and that the solute chemistry is expected to be in the dilute solution limit in which solute – solute interactions can often be neglected.

2 Literature Review

Chemical speciation in molten salt systems such as Li_2BeF_4, which is used as the coolant salt in the KP-FHR, can be estimated using thermodynamics if we assume the system reaches equilibrium on a timescale larger than that which represents the reaction kinetics. Because of high temperatures and the assumption of a well-mixed flowing salt, using thermodynamics alone in predicting the chemical state of the elements in the coolant can be assumed to be satisfactory, especially for those representations of the salt over a long period of time [1, 2]. A review of the thermochemistry of molten salt systems is provided here, along with a presentation of thermochemical data found in literature relevant to modeling speciation and evaporation in molten fluoride salts.

2.1 Thermodynamic Principles

The thermodynamics of nuclear fuels has been well documented in literature [1-4], therefore only a brief review is provided here. Although much of the literature is based on the thermodynamics of solid oxide fuels, many of the underlying phenomena, of which these thermochemical models are based on, also apply to ionic liquids such as molten salts.

Based on the laws of thermodynamics, the Gibbs free energy, G, of an isolated system at constant temperature and pressure must never increase. Therefore, chemical equilibrium of the system is attained when the change in G is equal to zero, or put simply, when G has reduced to its minimum value. This fundamental principle of thermodynamics is used to estimate the final composition of species in chemical systems based on some minimization of thermodynamic data representing the system and its components, i.e., the elements. Although a simple concept, its implementation for molten salt nuclear systems is not so trivial for several reasons, including constantly evolving species due to nuclear reactions, constantly changing temperature and pressure of the system, inaccurate or incomplete fundamental thermodynamic data for components, and effects of mixing. This report will only provide discussion on the thermochemistry of a system that is assumed to have constant elemental composition at a given temperature and pressure, relying on the fundamental definition of chemical equilibrium of a system. This assumption is expected to be accurate for the KP-FHR where solutes will be present in very dilute concentrations. In the dilute solution limit that is relevant to the FLiBe in the KP-FHR, small changes in solute concentrations can often be neglected because solute-solute interactions will not influence chemical equilibrium.

The Gibbs free energy of a system depends on temperature, pressure, and composition. Therefore, a general expression for the differential of G can be seen in equation 2-1, and can be simplified using the Maxwell relations to produce equation 2-2: [3]

$$dG = \left(\frac{\partial G}{\partial T}\right)_{p,n_j} dT + \left(\frac{\partial G}{\partial p}\right)_{T,n_j} dp + \sum_i \left(\frac{\partial G}{\partial n_i}\right)_{T,p,n_{j\neq i}} dn_i \qquad \textbf{2-1}$$

$$dG = -S\,dT + V\,dp + \sum_i \left(\frac{\partial G}{\partial n_i}\right)_{T,p,n_{j\neq i}} dn_i \qquad \textbf{2-2}$$

The chemical potential of species *i*, μ_i, can be defined as the partial derivative of the Gibbs free energy of the system with respect to the number of moles of species *i,* n_i. Chemical potential is also known as the partial molar Gibbs free energy:

$$\mu_i = \left(\frac{\partial G}{\partial n_i}\right)_{T,p,n_{j\neq i}} \quad \textbf{2-3}$$

The equilibrium composition in each phase of a multi-phase system at constant T and P can be found by searching for the global minimum of the Gibbs free energy of the system:

$$dG = \sum_i \mu_i \, dn_i = 0 \quad \textbf{2-4}$$

It follows that the phase equilibrium criterion for satisfying this expression is that the chemical potential of species *i* in one phase is equal to the chemical potential of species *i* in any other phase in equilibrium in the system: [5]

$$\mu_i{}^I = \mu_i{}^{II} = \mu_i{}^{III} = \cdots \quad \textbf{2-5}$$

where the superscripts denote a phase in the system. Similarly, it is worth noting there is also a chemical equilibrium criterion based on the chemical potentials being stoichiometrically constrained. More simply, a system is only in chemical equilibrium if the chemical reactions which may occur in this system are themselves also in equilibrium [5]. The equilibrium composition of a system can be found as long as these criteria, as well as the conservation of mass, are satisfied.

Many have reported methods of computational chemistry on the minimization of the Gibbs free energy of a multicomponent system, starting with White et al. in 1958 [6]. Explanations of the optimization procedure can be found in literature [7], but the concept is simply to find the composition of chemical species in each phase in a system of known elements at a set temperature and pressure which allows for the smallest value of G. This requires knowledge of the potential chemical species and potential phases which may be formed in this system of elements, and more importantly, the thermodynamic quantities representing the chemical potential of those species. Because there will always be the possibility of the formation of unknown chemical species, thermochemical modeling will always be only as accurate as the thermodynamic data of the theorized potential species. Historically, this has been experimentally measured data which is specific to the compound and the system in which it was measured, but the use of standard or reference states allows for the use of thermodynamic data of different experiments in the same optimization problem.

The chemical potential of a species in a system can be represented in a more physically convenient way by utilizing an equation-of-state such as the ideal gas law seen in equation 2-6. It is also convenient to define the mole fraction of a component in a solution of N components, x_i, as seen in equation 2-7:

$$pV = nRT \quad \textbf{2-6}$$

$$x_i = \frac{n_i}{\sum_{j=1}^{N} n_j} \quad where \quad \sum_{i=1}^{N} x_i = 1 \quad and \;\; x_i > 0 \quad \textbf{2-7}$$

For an ideal multi-component gas in a system at constant T, equation 2-2 can be expressed as: [3]

$$G_i(p_i) = G_i(p_i^\circ) + \int_{p_i^\circ}^{p_i} V_i \, dp_i \quad \textbf{2-8}$$

where p° is the reference pressure, typically 1 bar. Substituting in the ideal gas law, and noting the fact that the molar Gibbs free energy of a component in a multi-component ideal gas system is the same as the chemical potential of that component, the expression becomes:

$$\frac{G_i(p_i)}{n_i} = \frac{G_i(p^\circ)}{n_i} + RT \;\ln\frac{p_i}{p^\circ} \quad \textbf{2-9}$$

$$\mu_i(p_i) = \mu_i^\circ(p^\circ) + RT \;\ln\frac{p_i}{p^\circ} \quad \textbf{2-10}$$

where $\mu_i^\circ(p^\circ)$ is the standard chemical potential of the pure ideal gas of component *i* at the reference pressure. Dalton's law of partial pressures can also be substituted here to relate the mole fraction, x_i, to the chemical potential.

The chemical potential of a species in solid or liquid solutions has a similar form but is related to a newly defined quantity called the chemical activity, a_i (equation 2-11). The activity is related to the mole fraction of the component in solution by the activity coefficient, γ_i, which is a function of temperature, pressure, and composition (equation 2-12). Similar to above, μ_i° is the standard chemical potential of the pure component at the standard reference pressure p° with an activity value equal to one: [3]

$$\mu_i = \mu_i^\circ + RT \;\ln a_i \quad \textbf{2-11}$$

$$\gamma_i = \frac{a_i}{x_i} \quad \textbf{2-12}$$

For values of $\gamma_i > 1$, the system experiences a positive deviation from ideality, i.e., it is destabilized relative to an ideal solution. Conversely, if $\gamma_i < 1$, the system experiences a negative deviation from ideality and is comparatively more stabilized than the ideal case.

Deviations from ideality in liquid mixtures occur because of mixing effects. Thermodynamically, this can be represented by the Gibbs energy of mixing, which is the difference between the Gibbs energies of solution before and after mixing takes place. The initial Gibbs energy of solution is given by the stoichiometric sum of the Gibbs energies of the pure components of the solution, i.e., the end-members. The final Gibbs energy of the mixed solution is equal to the sum of the partial

molar Gibbs energies of each component ($\bar{G}_{m,i}$). The analogous mixing terms for enthalpy and entropy are defined similarly, and the subscript *m* refers to it being on a molar basis, sometimes stylized with a underbar:

$$\Delta_{mix}G_m = \Delta_{mix}\underline{G} = \sum_i x_i(\bar{G}_{m,i} - G_{m,i}) = \sum_i x_i(\mu_i - \mu_i^\circ) \quad \textbf{2-13}$$

$$\Delta_{mix}H_m = \sum_i x_i(\bar{H}_{m,i} - H_{m,i}) \quad \textbf{2-14}$$

$$\Delta_{mix}S_m = \sum_i x_i(\bar{S}_{m,i} - S_{m,i}) \quad \textbf{2-15}$$

Combining equations 2-11 and 2-13 provides us with the Gibbs energy of mixing as a function of the chemical activity:

$$\Delta_{mix}G_m = RT\sum_i x_i \ln a_i \quad \textbf{2-16}$$

For ideal mixtures, the activity and mole fraction are equal, so the Gibbs energy of mixing for ideal solutions becomes:

$$\Delta_{mix}G_m^{ideal} = RT\sum_i x_i \ln x_i \quad \textbf{2-17}$$

And applying the Maxwell relations to equation 2-17, the entropy and enthalpy of mixing for ideal solutions can be derived as well:

$$\Delta_{mix}S_m^{ideal} = -R\sum_i x_i \ln x_i \quad \textbf{2-18}$$

$$\Delta_{mix}H_m^{ideal} = \Delta_{mix}G_m^{ideal} + T\Delta_{mix}S_m^{ideal} = 0 \quad \textbf{2-19}$$

Unfortunately, most mixtures do not exhibit ideal behavior and, therefore, the difference between the real Gibbs energy of mixing and the ideal Gibbs energy of mixing is nonzero. This difference, termed the excess molar Gibbs energy of mixing (or just the excess molar Gibbs energy, sometimes stylized as $\underline{G}^{ex}$) is a function of the mole fractions and activity coefficients of the mixture:

$$\Delta_{mix}G_m^{excess} = \underline{G}^{ex} = \Delta_{mix}G_m - \Delta_{mix}G_m^{ideal} = RT\sum_i x_i \ln \gamma_i \quad \textbf{2-20}$$

The excess molar entropy and enthalpy of mixing can be found in a similar fashion:

$$\Delta_{mix}S_m^{excess} = \Delta_{mix}S_m - \Delta_{mix}S_m^{ideal} = \Delta_{mix}S_m + R\sum_i x_i \ln x_i \quad \textbf{2-21}$$

$$\Delta_{mix}H_m^{excess} = \Delta_{mix}H_m - \Delta_{mix}H_m^{ideal} = \Delta_{mix}H_m \quad \textbf{2-22}$$

The partial molar excess Gibbs energy of component *i* (stylized with an overbar to refer to a partial molar quantity) is defined as seen in equation 2-23. It follows that the partial molar excess Gibbs energy of component *i* is the difference between the partial molar Gibbs energies of component *i* in real and ideal mixtures, as seen in equation 2-24: [5]

$$\bar{G}_i^{ex} = \left(\frac{\partial(N\underline{G}^{ex})}{\partial N_i}\right)_{T,p,N_{j\neq i}} \quad \textbf{2-23}$$

$$\bar{G}_i^{ex} = \bar{G}_i - \bar{G}_i^{ideal} \quad \textbf{2-24}$$

It eventually follows that the partial molar excess Gibbs energy can be related to the activity coefficient: [5]

$$RT\ln\gamma_i(T,P,\underline{x}) = \bar{G}_i^{ex} = \left(\frac{\partial(N\underline{G}^{ex})}{\partial N_i}\right)_{T,p,N_{j\neq i}} \quad \textbf{2-25}$$

It is reiterated that the excess Gibbs energy can also be estimated from values of enthalpy of mixing and excess entropy of mixing, if these are known from experiment. This would lead to calculation of the activity coefficient of the component in the solution. Also, if a system can be represented by an equation for the excess molar Gibbs energy as a function of composition, an equation for the activity coefficient can be found as a function of temperature, pressure, or composition. The Gibbs-Duhem equation for activity coefficients eventually follows from this as a result for a binary mixture, relating both activity coefficients and both corresponding mole fractions: [5]

$$x_1\left(\frac{\partial\ln\gamma_1}{\partial x_1}\right)_{T,p} + x_2\left(\frac{\partial\ln\gamma_2}{\partial x_1}\right)_{T,p} = 0 \quad \textbf{2-26}$$

2.1.1 Phase Equilibrium

The discussion above introduces the concepts and formulas relevant to the mixing of pure components to form non-ideal solutions and how that affects the resulting solution's thermodynamic properties, often represented by the excess chemical potential, or partial molar excess Gibbs free energy. The use of this information in predicting phase equilibrium can be discussed.

The vapor pressure of dilute solutions can be described using either Henry's law or Raoult's law, which approximate the vapor pressure of the dilute solute or the solvent which contains the solute, respectively. For a dilute solution of solute B in solvent A, Henry's law states that the partial pressure of B above a solvent A is directly proportional to the concentration of the solute,

where $k_{H,B}$ is called Henry's constant of solute B in solvent A, as seen in equation 2-27. Henry's constant is dependent on the solute-solvent pair, temperature, and pressure. Similarly, for dilute solutions, Raoult's law states that the vapor pressure of solvent A is given by the product of the vapor pressure of the pure component, p_A^*, and the mole fraction of A, as seen in equation 2-28.

$$p_B = x_B \, k_{H,B} \tag{2-27}$$

$$p_A = x_A \, p_A^* \tag{2-28}$$

It is worth noting here that Henry's law and Raoult's law (equations 2-27 and 2-28) are special relationships of fugacity which are derived for systems where the total pressure and the vapor pressure of the species are sufficiently low such that all fugacity coefficient corrections are negligible [5]. Similar to the concept of activity for a solute in a liquid solution, the concept of fugacity represents a solute's gas phase interactions and is a function of the difference between the real and ideal gas phase Gibbs energies [5]. Raoult's law is a result of this found by equating the fugacities of the solute in each phase. For systems with low pressures and high temperatures, the fugacity of the pure species as a pure liquid is approximately equal to the pure component vapor pressure and the fugacity of the species in the vapor phase of the mixture is equal to its partial pressure. This is especially true for nuclear molten salt systems, such as in the KP-FHR, which are not only at relatively low pressures, but also at high temperatures, which both allow for a fugacity coefficient typically close to unity. In the case of supercritical fluids where the estimated value of vapor pressure is found by extrapolating beyond the critical point, resulting in very high vapor pressures, it may not be sufficient to estimate a fugacity coefficient of unity [5].

Real solutions follow these laws only at infinite dilution, i.e., as $x_B \to 0$ and as $x_A \to 1$. For other (nonideal) solutions, activity coefficients are used to represent the Henrian and Raoultian standard states. Activity coefficients, like activity, are dependent not only on composition, but also on temperature and pressure:

$$\gamma_B^H = \frac{a_B^H}{x_B} \tag{2-29}$$

$$\gamma_A^R = \frac{a_A^R}{x_A} \tag{2-30}$$

The subscripts A and B refer to the solvent and solute, respectively, and the superscripts H and R refer to standard states under Henry's law and Raoult's law, respectively. These reference standard states occur at infinite dilution, as described above, so that $\gamma \to 1$, therefore, the Henrian reference state is hypothetical ($x_B \to 0$). The chemical potential can be described using either reference state:

$$\mu_i = \mu_i^{R\circ} + RT \ \ln a_i^R = \mu_i^{H\circ} + RT \ \ln a_i^H \tag{2-31}$$

Henry's law and Raoult's law can be used for real, or nonideal, solutions (which don't represent infinite dilution of the solute or nearly pure composition of the solvent) with the addition of the respective activity coefficient: [5]

$$p_B = x_B \, k_{H,B} \, \gamma_B^H \quad \textbf{2-32}$$

$$p_A = x_A \, p_A^* \, \gamma_A^R \quad \textbf{2-33}$$

For the same component in solution, these two laws can be equated, being cognizant of the need for both activity coefficients if the system is not at one end of the extremes of the solute mole fraction. Otherwise, only one of the activity coefficients is needed, such as in the case of a very dilute solution of solute B in solvent A. In this case, Henry's law will be in the ideal form, but Raoult's law will require the use of γ_A^R to account for the dominating effect of solute-solvent interactions in replace of the effect of solute-solute interactions, which would otherwise be assumed to dominate under Raoult's law (i.e., when solute B is in large concentrations relative to the solvent). The following equation shows the relation between Henry's constant and the pure component vapor pressure and the Raoultian (traditional) activity coefficient for very dilute volatile component B in a liquid mixture:

$$k_{H,B} = p_B^* \, \gamma_B^R \quad \textbf{2-34}$$

Additionally, one can define a vapor-liquid equilibrium constant as the ratio of the mole fraction of the solute in the vapor phase to that in the liquid phase. By rearranging Raoult's Law (equation 2-28), one can find a formula for the vapor-liquid equilibrium constant, which is typically a function of temperature:

$$K_{d,i} = \frac{y_i}{x_i} = \frac{\gamma_i^R p_i^*}{p} \quad \textbf{2-35}$$

where p is the total pressure of the system. This relation can be used to relate the liquid and vapor phase mole fractions of the solute.

In summary, phase equilibria can be approximated using relations for the fugacity of a solute in a mixture, most commonly with Raoult's law and a correction factor termed the activity coefficient which is found experimentally, or estimated from solution models, which are also typically informed by experiment as well as theory. It has also been mentioned that an isolated system will maximize its entropy and minimize its free energy [1]. As will be shown later, this provides some reasoning as to why negative deviations from ideality occur for mixtures with values of increasing entropy of mixing and decreasing enthalpy of mixing. A negative deviation from ideality can be physically represented by a more thermodynamically stable system with a reduced vapor pressure, i.e., components that are more comfortable in the molten solution phase than not.

2.2 Molten Salt Thermochemistry

Despite often having thermophysical properties resembling that of aqueous solutions, molten salts are represented by different thermochemical models based on their structure as well as a lack of the dominating forces of hydrogen bonding which are seen in water. Molten salts are solutions made up of cations and anions situated in a fluid lattice which experience simultaneously the

opposing forces of attraction and repulsion from nearby neighbors. The result of this is that coulomb interactions largely influence the energetics and major properties of molten salts [8].

Broadly speaking, one can describe the solution properties of a multicomponent molten salt mixture based on two fundamental types of information: [8]

1. The magnitude of the basic interactions between the ions of different components
2. Methods for incorporating information on interactions into a complete description of multicomponent systems

The first type of information is difficult to estimate theoretically but is typically contained in the binary system thermodynamic data for each combination of component pairs in a multicomponent system. This experimental data is necessary to deduce the properties of higher order systems and forms the starting point for estimating the thermochemistry of all molten salt systems. Examples of forms of binary system data include phase diagrams, interaction parameters, thermodynamic quantities, activity coefficients, or others. While a lack of certain binary system data does not preclude the possibility of arriving at reasonable estimations of thermodynamic properties of a multicomponent system, it certainly adds to the uncertainty.

The second type of information needed involves the methods that utilize the binary system data to make predictions for the higher order systems (e.g., ternary, quaternary, etc.) These calculations are based on physical models and statistical mechanical methods. These methods have been shown to produce seemingly accurate thermodynamic properties of solutions just by utilizing that basic interaction data and extrapolating to more complex systems within the framework of the theorized physical model. The extent to which this has been developed thus far will be briefly summarized in this section.

2.2.1 Research During ORNL MSR Programs

Much salt thermochemistry research was completed at ORNL in the mid 20th century as part of the seminal MSR programs: the Aircraft Nuclear Propulsion Program (ANPP) and later the Molten Salt Reactor Program (MSRP). Some of the research that occurred during these programs which is relevant to modeling the thermochemical properties of molten salts is highlighted here.

In 1957, Blander stressed the importance of salt thermochemistry to molten salt fuel mixture design, noting how adding a component to a mixture would impact the properties of the solution. With the goal of understanding changes in the solubility of fuel salt components (as compared to an ideal solution), he proposed a relation for determining activities of the precipitating phase from a molten solution. Noting that the activity of a salt as a solid is equal to its activity in solution at the freezing point, he related the mole fraction and activity coefficient of a component in a mixture, and the freezing point of the mixture (or alternatively, the solubility of the component in the mixture), with the heat of fusion and melting point of the pure component. For most mixtures, this only requires experimental data on the liquidus temperature or freezing point (or solubility) for a component in a mixture to be able to estimate the activity coefficient of that component in solution: [9]

$$\ln a_i = \ln \gamma_i + \ln x_i = \frac{-\Delta H_{fus}}{R}\left(\frac{1}{T} - \frac{1}{T_0}\right) \quad \textbf{2-36}$$

where ΔH_{fus} and T_0 are the heat of fusion and melting point of the pure component salt, respectively. T is the freezing point of the mixture, or can also represent the temperature at which solubility is reached for a component in the mixture. If a large temperature range is used, the equation must be modified because of the change in the heat of fusion over a wide range of temperatures [9].

For all fluoride salt components and mixtures tested up until this point, Blander notes that no fluoride salt solution has exhibited ideal behavior, adding there is always a negative deviation from ideality ($\gamma_i < 1$).

This presumably only corresponds to cations in fluoride salt solutions, and not for a second anion such as iodide in a reciprocal system with fluoride ions. He continues to note that the degree to which the solution deviates from ideality is chiefly dependent on the difference in the value of the charge-to-radius ratio (Z/r) for the cations involved:

> *"The extent of reduction of the activity, given by the activity coefficient, is more pronounced the larger the difference in the charge-to-radius ratios, Z/r, for the cations in the mixture."*

Equation 2-36 and experimental solubility data were used in this work to estimate activity coefficients of several cations in binary fluoride mixtures. The reported data for LiF in a binary system with NaF, KF, RbF, or ZrF_4 are shown in Table 2-1 below [9]. It can be easily shown that the activity coefficient is greatly reduced for systems where the two cations are very different in charge-to-radius ratio (e.g., LiF-ZrF_4).

Table 2-1: Activity Coefficients of LiF in Several Binary Fluorides [9]

Temperature (°C)	LiF-NaF		LiF-KF		LiF-RbF		LiF-ZrF_4	
	N*	γ*	N	γ	N	γ	N	γ
500			0.51	0.53	0.54	0.50		
600			0.61	0.72	0.64	0.69	0.79	0.56
700	0.68	0.94	0.74	0.87	0.76	0.85	0.85	0.76
800	0.90	0.97	0.91	0.96	0.91	0.96	0.94	0.94

*N is the mole fraction of LiF, and γ is the activity coefficient of LiF.

Blander notes that the reduction in freezing points cannot be solely explained by this phenomenon, and compound formation frequently complicates the picture for the central portions of the phase diagrams, but the charge-to-radius ratio still appears to be a predominant factor in understanding the effect on freezing points [9].

The cause for deviations from ideality is analyzed based on the thermodynamic principles which were covered in the previous section. Blander correctly notes that the activity coefficient and the

excess free energy of mixing can be related by equation 2-25 along with the relationship for Gibbs free energy, enthalpy, and entropy, also utilizing equations 2-14 and 2-22: [9]

$$\ln \gamma_i(T,P,\underline{x}) = \frac{\bar{G}_i^{ex}}{RT} = \frac{\bar{H}_i^{ex}}{RT} - \frac{\bar{S}_i^{ex}}{R} = \frac{\overline{H}_i - H_{m,i}}{RT} - \frac{\bar{S}_i^{ex}}{R} \qquad \textbf{2-37}$$

The activity coefficient is thus a function of two terms: the partial molar enthalpy of mixing and the partial excess molar entropy of mixing. We can also see that the effect of temperature on the activity coefficient is dependent on having a significant enthalpy of mixing term.

The impact of this is discussed later as we will see that sometimes the entropy term dominates and therefore the activity coefficient may not vary much with temperature. Nonetheless, deviations from ideality can be explained by the effect that mixing the pure components has on both the enthalpy of the solution and the excess entropy of mixing: [9]

> *"Activity coefficients less than unity can result from negative heats of solution or from positive excess entropies. In other words the ions in solution must have a lower heat content than they have when unmixed, and the mixing must result in a larger amount of 'disordering' (i.e., a larger number of configurations of equivalent energy than is the case with random mixing) than results from the formation of an ideal solution…"*

As mentioned previously, molten salts can be viewed as a flexible lattice of charged balls consisting of cations and anions alternating as necessary to allow for the electrostatic forces between neighbors. This results in significantly more ordering than something like an aqueous solution might experience during random mixing. Consider a binary system of NaF and KF where Na and K cations interpenetrate the fluoride lattice. Although these two cations may not be "comfortable" in each other's cation spot in a rigid crystal lattice, a liquid lattice is a more flexible lattice with a lack of long-range ordering and finds the most "comfortable" configuration of the cations with the lowest energy. The resulting mixed lattice provides a configuration with lower energy than the average energy of the unmixed lattices:

> *"The lower energy configurations give rise to negative heats of solution. As an example of the factors contributing to this, it can be shown that the electrostatic repulsion between nearest cations is less when large and small cations alternate than the overage of the repulsions between small cations and large cations among their own kind. The difference is more pronounced the greater the difference in cation size, and similarly the negative heat of solution increases."*

Additionally, the lattice of mixed cations experiences warping due to this now lower energy configuration, therefore it is distorted from initial configurations of the pure components which increases "disorder" and thus increases the excess entropy of mixing. This higher entropy of mixing value goes beyond that which represents a lattice of the same cation which would experience disordering from mixing without lattice distortion:

> *"The resulting excess entropy of mixing will be greater for more pronounced warping, and the amount of warping increases with the difference in cation size. This explains the source of the positive excess entropies of mixing."*

These two effects (enthalpy of mixing and excess entropy of mixing) go hand-in-hand, although typically one value dominates. As Blander points out, negative deviations from ideality are often misrepresented as results of complex formations [9]. While the formation of complex ions (also known as associating species) represents a large excess entropy term, especially for lattices with cations of different charges, the enthalpy term is often the larger contributor to the negative deviation for lattice of the same cation charge.

> *"There is a prevalent practice of ascribing all negative deviations to complex formation. This places the emphasis on the entropy term and lattice distortions and causes the heat effect to be ignored, and, in the extreme view, it leads to the statement that NaF is complexed by KF because Na^+ ions have more attraction for the fluoride ion than do the K^+ ions. This statement is not wrong, but it implies a much less restricted definition of 'complex' than is usually intended."*

Nonetheless, not all deviations can be explained by the heat effect, and not all entropy-induced deviations can be explained by the differences in the Z/r ratio. Complex formation does account for a large excess entropy of mixing term at times, such as in the NaF-ZrF_4 solution, where there is a definite preference by the fluoride ions to position as neighbors of the Zr^{4+} ions. Although the charge-to-radius ratio typically predicts the trend in thermochemical properties (e.g., freezing point lowering), this is an instance in which complex formation (influenced more by charge than by size) dominates the effect on activity.

During these research programs, the total and partial pressures of many compounds and mixtures were measured. Cantor estimated activity coefficients of ZrF_4 in a NaF-ZrF_4 binary mixture based on the assumption that ZrF_4 was the only volatile species in the mixture by comparing total pressure of the mixture to the pure component vapor pressure [9]. An empirical correlation was found which represents the logarithmic relationship between the activity coefficient of ZrF_4 and the mole fraction of ZrF_4. Assuming the correlation was valid for all compositions in the binary mixture at constant T and P, they were able to find the analogous correlation for the activity coefficient of NaF in the mixture by using the Gibbs-Duhem equation for activity coefficients (equation 2-26).

They note that the analogous equation was not valid for systems/compositions where complex formation was postulated because of the assumptions used. This nonetheless provides another method of estimating activity coefficient data when such data is only available for one component in a binary mixture. As mentioned above, both of these components in this binary fluoride had activity coefficients below unity, decreasing further with mole fraction.

The effect of partially substituting UF_4 for ZrF_4 in this binary mixture was investigated next, by forming a quasibinary mixture of $7NaF$-$6ZrF_4$-$7NaF$-$6UF_4$ [9]. The composition of UF_4 was increased (and the composition of ZrF_4 was decreased equivalently) in steps by adding $7NaF$-$6UF_4$ to a solution of $7NaF$-$6ZrF_4$, keeping the mole fraction of NaF in the "binary" constant. This allowed for a stepwise analysis of the effect on vapor pressure of replacing the more volatile ZrF_4. The slopes of the vapor pressure curves also allowed for determination of heat of vaporization, and it was found that if the slight differences in slope are neglected, nearly similar

values of heat of vaporization are found which means that replacing ZrF_4 with UF_4 did not provide an appreciable heat of mixing [9]. This can be seen in Figure 2-1 below, where the curve is fit for all the data points at all temperatures [10]. As noted previously, this means there is little change in activity of ZrF_4 with temperature for this system.

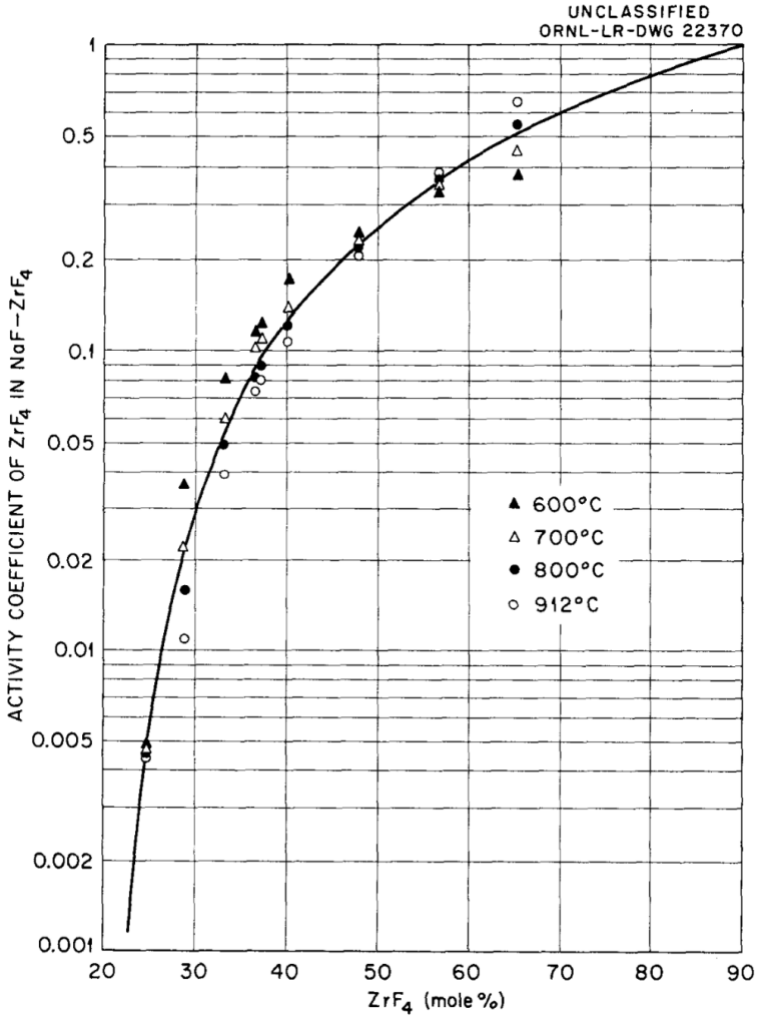

Figure 2-1: Approximate activities of ZrF_4 in NaF-ZrF_4 based on vapor pressure data [10]

Surprisingly, another result of this study was a decrease in the activity of ZrF_4 in this system (compared to the NaF-ZrF_4 system) for increasing UF_4 mole fraction, meaning the activity coefficient is less than 1 not just when comparing the activity of ZrF_4 to its pure component system, but also when comparing it to the even-more stabilized NaF-ZrF_4 system.

> *"The effect of the UF_4 can be interpreted to be that of an additional supply of fluoride ions for the complexing of ZrF_4. The vapor pressure is accordingly reduced to a greater extent than would have been the case if UF_4 and ZrF_4 had equal attractions for fluoride ions."*

This is compatible with previous data they obtained showing that UF_4 has a lower activity coefficient in alkali fluoride mixtures without ZrF_4 than in mixtures that do contain it [9]. It is postulated that the addition of UF_4 stabilizes the ZrF_4 in solution, but slightly destabilizes itself (relative to if no ZrF_4 was present). They note that this diminishes the vapor problem for ZrF_4 but

does not have as large of an impact on activity as would increasing the alkali fluoride mole fraction in the system (i.e., decreasing the ZrF_4 mole fraction).

As mentioned previously, the thermochemical stability of a salt system can be explained by the charge-to-radius ratios (Z/r) of the components in the lattice, which is a direct measure of the coulombic force between neighboring ions.

The larger the difference between the Z/r values of cation neighbors, the more stable the configuration becomes. Even for binary systems with two cations of the same coordination (charge) and with little distortion, there is still a stabilizing effect felt due to a decrease in cation repulsive energy upon mixing. This is shown in Figure 2-2 where it can be seen that the enthalpy of mixing, which is proportional to the change in charge-to-radius ratios of each cation pair, is negative for a system of mixed cations such as LiF-KF [11]. This effect is heightened for systems with cations of different charge, cations with larger differences in size, and systems with associating cations.

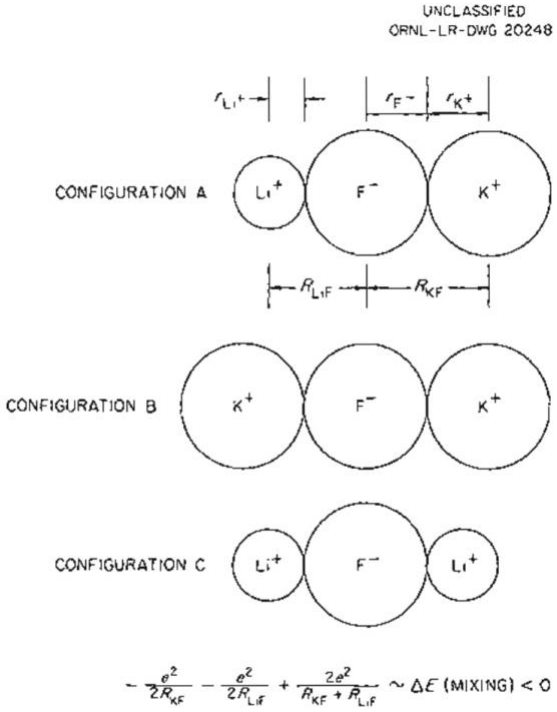

Figure 2-2: Diagram of cation repulsion energies for various ion configurations showing the gain in stability upon mixing [11]

Continuing with the example of the $NaF\text{-}ZrF_4$ system, the effect of the charge-to-radius ratio on the nonideal behavior of solutes in a solvent can be explained [11].

Each component, or cation-anion pair, in the mixture is represented by a Z/r ratio. The solvent can be represented by an effective Z/r ratio, which is some intermediate value, typically close to but not necessarily exactly the average, between the two end-members of the mixture.

If the *Z/r* ratio of a solute added to the solvent is the same as the effective *Z/r* ratio of the solvent, this composition of the solvent is termed the "neutral composition", which is where the activity coefficient of that solute is at a maximum [12]. For solutes with *Z/r* ratios far from the effective *Z/r* ratio of the mixture, or similarly, if the composition of a solvent is chosen so that the effective *Z/r* ratio is far from the *Z/r* ratio of a specific solute, then the solute will experience a reduced activity coefficient than if the two *Z/r* ratios were closer together in value.

For a mixture of $2NaF\text{-}ZrF_4$, the effective *Z/r* ratio is somewhere between that for NaF (*Z/r* = 0.43) and ZrF_4 (*Z/r* = 1.82). The addition of UF_4 (*Z/r* = 1.68) to the mixture increases the effective *Z/r* ratio, thereby lowering the activity coefficient of NaF and increasing it for ZrF_4. This is evidenced by an increase in the vapor pressure of ZrF_4 when going from the $2NaF\text{-}ZrF_4$ system to the $2NaF\text{-}ZrF_4\text{-}UF_4$ system. Even more surprising is the fact that the latter system contains a smaller mole fraction yet has a higher vapor pressure for ZrF_4.

Alternatively, effective *Z/r* ratio can be used to explain the anomalous behavior seen for the $7NaF\text{-}6ZrF_4\text{-}7NaF\text{-}6UF_4$ system previously mentioned. These mixtures were formed by adding UF4 in a way which does not alter the mole fraction of NaF, partially substituting some of the ZrF_4 end-members with UF_4 end-members. This is a noteworthy distinction, because instead of increasing the effective *Z/r* ratio of the mixture as in the previous system, replacing a component with a lower *Z/r* ratio and keeping everything else the same serves to lower the effective *Z/r* ratio. This means the vapor pressure of ZrF_4 should not only be reduced, but it should be reduced more sharply than just due to the reduction in mole fraction in the mixture. This is precisely what was seen experimentally [11].

Fluoride salt mixtures can further be described in terms of their fluoroacidity [11]. For example, the $NaF\text{-}ZrF_4$ system contains one cation end-member (Na^+) that is typically a fluoride donor (basic), and one cation end-member (Zr^{4+}) that is typically a fluoride acceptor (acidic). Evidence supporting the highly acidic character of the zirconium end-member includes the cation's preference in forming ZrF_7^{---} complex ions, where maximum complex formation understandably occurs at the stoichiometry $3NaF\text{-}ZrF_4$. The tendency of the sodium cation to "donate" its fluoride ion to a neighboring zirconium ion demonstrates its basic character and allows for a very stable solvent mixture.

> *"The stronger the acid and the base that are combined, the stronger they complex each other on mixing, or stated in thermodynamic terms, the greater are the negative deviations from ideal solution behavior shown by the mixture."*

The fluoride ion activity can be correlated by an acid-base scale based on the *Z/r* ratio of the end-member, where acidity increases with the ratio. By marking the points on the left and right ordinates of a figure corresponding to each end-member's *Z/r* ratio, and connecting the two points, a curve representing the potential effective *Z/r* ratio can be found. Unfortunately, the real effective *Z/r* ratio is probably not a straight line and requires more data points to fill out the curve. As an example, Hill and Blankenship conclude that because FeF_2 behaves ideally in the $NaF\text{-}ZrF_4$ (53-47 mol%) system, this composition must represent the neutral composition at the *Z/r* ratio for FeF_2. This is a 3rd data point which can be marked on the figure, as seen in Figure 2-3. The authors also note that because the liquid structure probably changes at 25 mol% ZrF_4, this is where the curve probably has maximum curvature. They later reported preliminary results

showing an increase in activity coefficient of a solute NiF_2 in NaF-ZrF_4 as the composition of the mixture, and thus the effective Z/r, became closer in value to that of the solute. This is where they predict the activity coefficient would be at a maximum, although their experiment is not complete, and this was not confirmed [13]. They note that this is simply a qualitative and potentially incomplete method of correlating solute and solvent characteristics (Z/r ratio) with predicted thermochemical behavior: [11].

> *"The purpose of such plots is to aid in predicting the relative acidity or basicity of a solute toward a solvent. This permits estimates of the relative negative deviations of solutes and, hence, also relative solubilities in case the pure solute is the saturating phase. An important use is the selection of solvent compositions which will reduce corrosion by complexing the corrosive agents rather than the corrosion products. Because of uncertainties in theory, ion radii, and neutral compositions, the plot is subject to revision."*

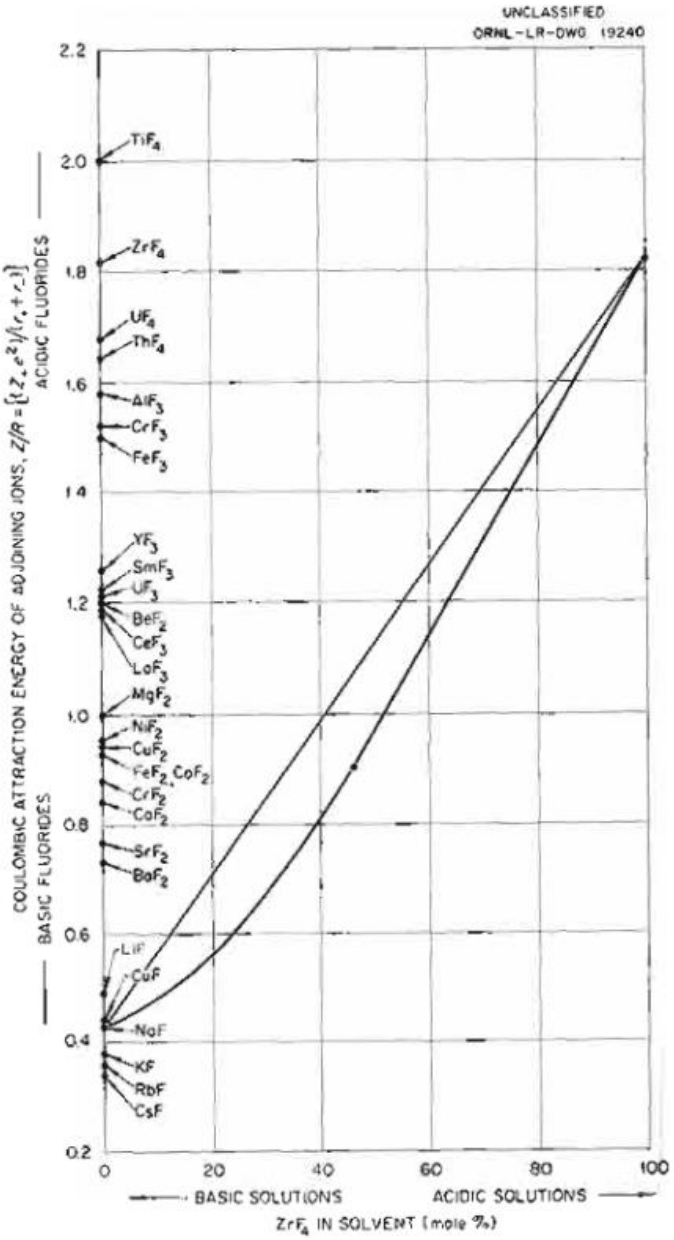

Figure 2-3: An acid-base scale for predicting neutral points of solutes in NaF-ZrF_4 melts [12]

Many studies were completed at ORNL during ANP in estimating the vapor pressures of fuel mixtures containing ZrF_4 because it was assumed the total pressure above the mixture was composed entirely of vapor phase ZrF_4 [9-13]. Unfortunately for BeF_2-containing systems, the vapor pressures of end-members of a mixture are experimentally more difficult to approximate because of the formation of various complexes [13]. Therefore, it is necessary to measure partial pressures of individual vapor phase compounds to be able to calculate activities of components in these systems.

Cantor and Ward later approximated activity coefficients of ZrF_4 over all mole fractions in the LiF-ZrF_4 binary mixture [14]. They combined two estimation techniques by (1) measuring the total pressure of the system for $x_{Zr} > 0.2$ and (2) using liquidus temperatures to estimate the activity coefficient of LiF for $x_{Zr} < 0.2$, combining with Gibbs-Duhem to solve for the activity coefficient of ZrF_4. The eutectic point of this binary is near $x_{Zr} = 0.2$. They used equation 2-38 to solve for the activity coefficient of LiF in this region of the binary:

$$-R \ln \gamma_i x_i = \left[\Delta H_{fus} - \left(C_{p,i}^L - a\right)T_m + \frac{b}{2}T_m^2 + \frac{c}{T_m}\right]\left(\frac{1}{T} - \frac{1}{T_m}\right) + \left(C_{p,i}^L - a\right)\ln\frac{T_m}{T} - \frac{b}{2}(T_m - T) + \frac{c}{2}\left(\frac{1}{T_m^2} - \frac{1}{T^2}\right) \quad \textbf{2-38}$$

where ΔH_{fus} is the heat of fusion of LiF at melting point T_m; $C_{p,i}^L$ is the molar heat capacity of liquid LiF; T is the liquidus temperature of the mixture; and a, b, and c are constants in the heat capacity equation for solid LiF in the form $C_{p,i}^S = a + bT - {}^{c}/_{T^2}$. They assumed γ_i is temperature-independent in this composition range due to negligible partial molar heat of solution, and thus with the Gibbs-Duhem relation in the form of equation 2-39, the activity coefficient of ZrF_4 was found, as seen in Figure 2-4.

$$d \ln \gamma_{Zr} = -\frac{x_{Li}}{x_{Zr}} d \ln \gamma_{Li} \quad \textbf{2-39}$$

As discussed above, the activity of a solute in a solution can be related to the change in freezing point (difference between liquidus and pure component melting point) of the dissolved solute. Therefore, studies on freezing-point depressions in sodium fluoride mixtures were conducted to better understand the thermochemistry effects of adding solutes to molten fluoride salt systems.

The first study tested the effect of cation size. This was investigated by adding the divalent alkaline earth cations to NaF up to 25 mol% solute [15]. It was shown that freezing-point depression increased as the cation radii decreased, where the freezing-point lowering of mixtures with the same solute mole fraction was in the order $BeF_2 > MgF_2 > CaF_2 > SrF_2 > BaF_2$. This was also shown (Figure 2-5) for trivalent cations where the same trend is seen with increasing freezing-point depression for decreasing cation radii: $AlF_3 > YbF_3 > YF_3 > DyF_3 > NdF_3 > LaF_3$ [16].

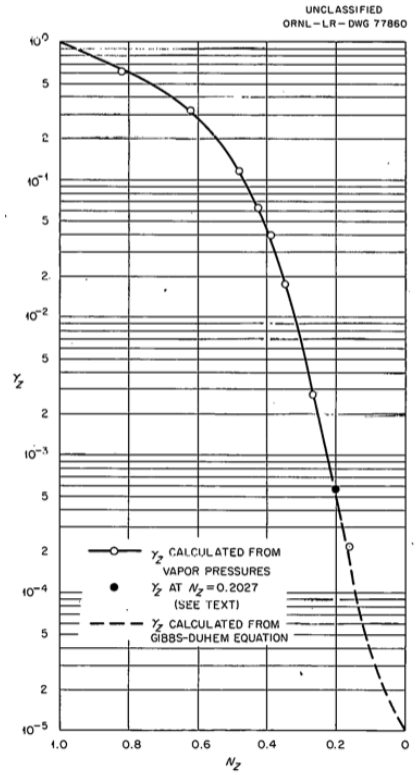

Figure 2-4: Activity coefficient of ZrF_4 vs mole fraction in the LiF-ZrF_4 system at 1000 K [14]

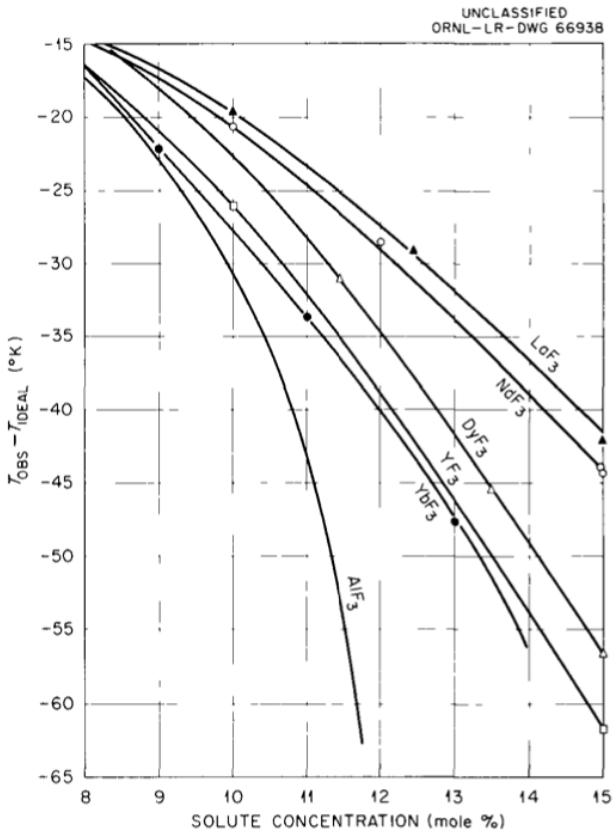

Figure 2-5: Deviation from ideal freezing-point depressions by trivalent metal fluorides in NaF [16]

Surprisingly, the opposite trend was seen for several tetravalent cations investigated in binary systems with NaF. The freezing-point lowering followed the order $ThF_4 > UF_4 > HfF_4 = ZrF_4$. This trend is opposite to that seen for the divalent and trivalent cations mentioned above, indicating the mechanism is probably more complex than just having a dependence on size, but rather it is dependent on some combination of size, charge, polarizability, and electronegativity. It was postulated that the larger tetravalent cations pull the fluoride ions closer, making it more difficult for NaF to establish long-range order and crystallize, allowing the mixture to be a liquid at lower temperatures: [17]

> *"This behavior is consistent with the assumptions that eightfold coordination of the tetravalent cation exists in solution (as it does in the crystalline state) and that the cation size determines the extent to which all eight fluoride ions are in contact with the cation. As the tetravalent ion size increases, more fluoride ions will be in contact, and, therefore, greater work will be required for the sodium ions to attract fluorides and establish long-range order, that is, crystallize. In fact, it is only in the case of Th^{4+} that all eight fluorides can have points of contact."*

The effect of cation charge was investigated by adding the fluoride salts of Ca^{2+}, Y^{3+}, and Th^{4+} to NaF, each constituting a cation of similar size as Na^+ but with different valence: [17]

> *"It is clear from the results indicated in [Figure* 2-6*] that the larger the cation charge of the solute, the greater its freezing-point depression. Stated differently, the stronger the electric field of the solute cation, the greater will be its attraction for fluoride ions, which, in turn, will make the establishment of long-range order for NaF (crystallization) more difficult."*

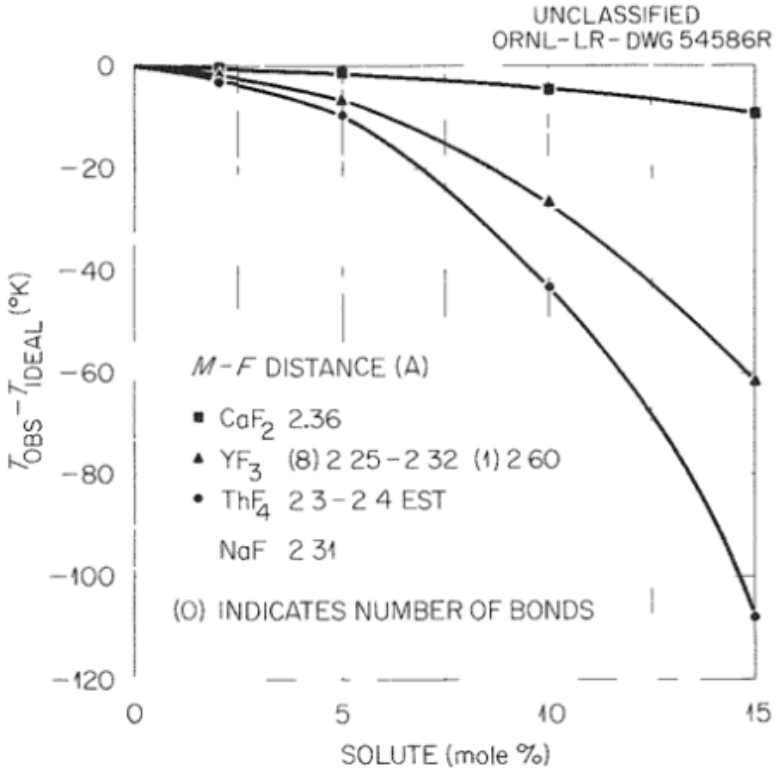

Figure 2-6: Freezing-point depressions in NaF caused by CaF_2, YF_3, and ThF_4 [17]

They also investigated the effect of polarizability by comparing the freezing-point depressions that occur when adding cations with similar size and valence (MgF_2 and ZnF_2) but different polarizabilities: [17]

> *"For MgF_2, and ZnF_2, whose cation sizes and charges are about the same, a significant structural difference is the greater polarizing power of the d^{10} electronic configuration (Zn^{2+}) over that in the inert-gas configuration (Mg^{2+}). Re-examination of the data shows that, indeed, as revealed by [Figure 2-7], ZnF_2 does depress the NaF freezing point somewhat significantly more than does MgF_2."*

The same trend is seen for the similarly sized InF_3 and ScF_3 which were added as solutes to NaF, each having a valence of 3+, as well as the similarly sized divalents, CaF_2 and CdF_2. The cations with the greater polarizability (In^{3+} and Cd^{2+}) were shown to have a more negative deviation from ideality [14].

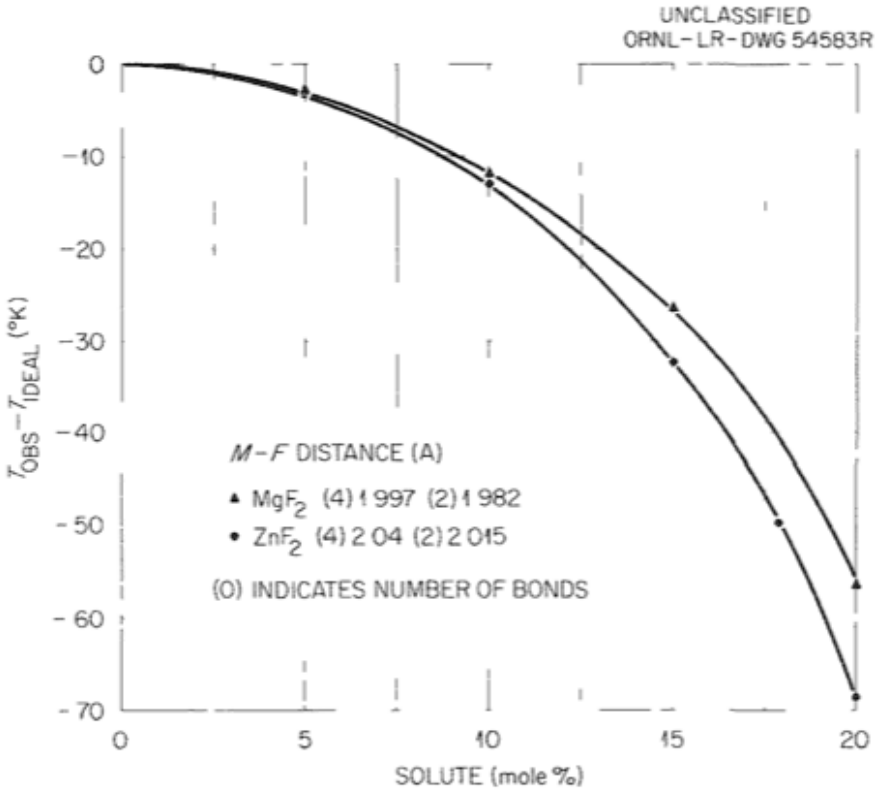

Figure 2-7: Freezing-point depressions in NaF caused by MgF_2 and ZnF_2 [17]

Binary solutions of NaF with fellow alkali cations show that it is possible to obtain positive deviations from ideality for fluoride salt mixtures [16]. The resulting freezing point of a mixture of NaF with CsF, RbF, or KF increased rather than being lowered, as seen in Figure 2-8. This was rationalized by considering the effect of London dispersion forces between next-nearest neighbors. When an alkali cation with a large polarizability (e.g., Cs^+) is added to one with a small polarizability (e.g., Na^+), the net change in dispersion energy will be positive. These increasing positive dispersion energies for CsF > RbF > KF follow the same order of the partial molal free energies of mixing in a NaF mixture, although a more detailed understanding of the interatomic forces may be needed to confirm this mechanism.

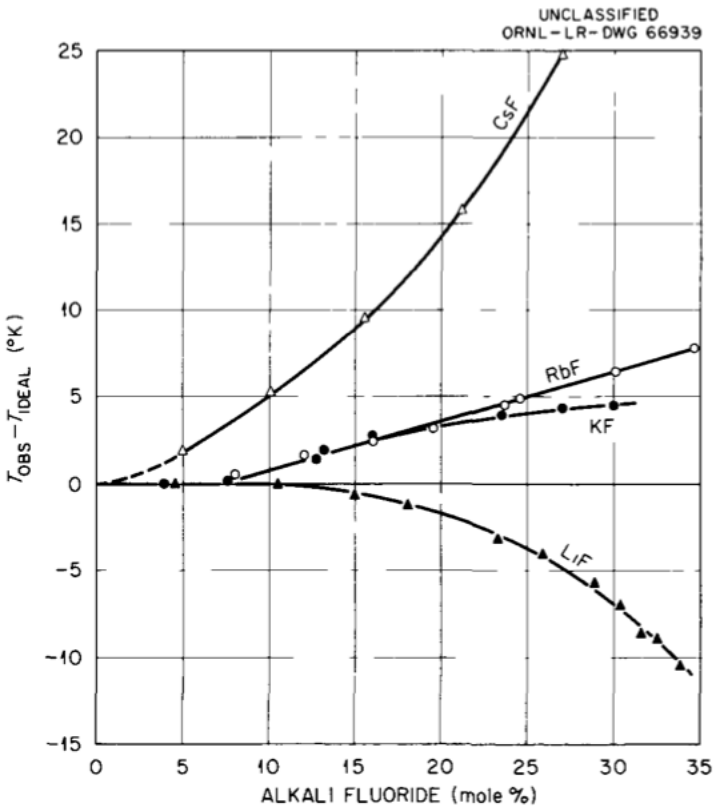

Figure 2-8: Deviation from ideal freezing-point depressions by alkali fluorides in NaF [16]

As mentioned above, the results may be correlated empirically in terms of the charge-to-radius ratio. The greater the difference between this ratio for the solute and the solvent (NaF, in this case), the greater the deviation from ideality. In this system, if Z/r for the solute is less than that of NaF, the deviation is positive, and if greater than that of NaF, the deviation is negative. This empirical rule is consistent with all the uni-, di-, and trivalent cation fluorides that were dissolved in NaF. The four tetravalent fluorides tested only partially followed this rule, as shown above, therefore further investigation is needed to confirm the underlying mechanism.

The relative contributions from London dispersion forces (represented by polarizability) and coulombic forces (represented by cation charge-to-radius ratio) can be better understood by comparing the NaF system containing alkali cation solutes with the LiF system containing alkali cation solutes [16]. As seen in Figure 2-9, the deviations from ideality are negative for all alkali solutes that are added to a LiF solvent mixture. Because the difference in Z/r is greater between NaF and LiF (LiF is considerably larger), the impact of the coulombic force between LiF and the other alkali solutes is a greater contributor to a negative deviation from ideality than is the positive contribution to a deviation from ideality by the large London dispersion forces. In other words, Li^+ and Na^+ have relatively close values of polarizability when compared to the larger alkali cations, so the difference in the contribution of London dispersion forces between these two systems is small. But because LiF has a much smaller effective ionic radius than NaF, the contribution from the coulombic forces from the even larger alkali solutes outweighs the London dispersion forces.

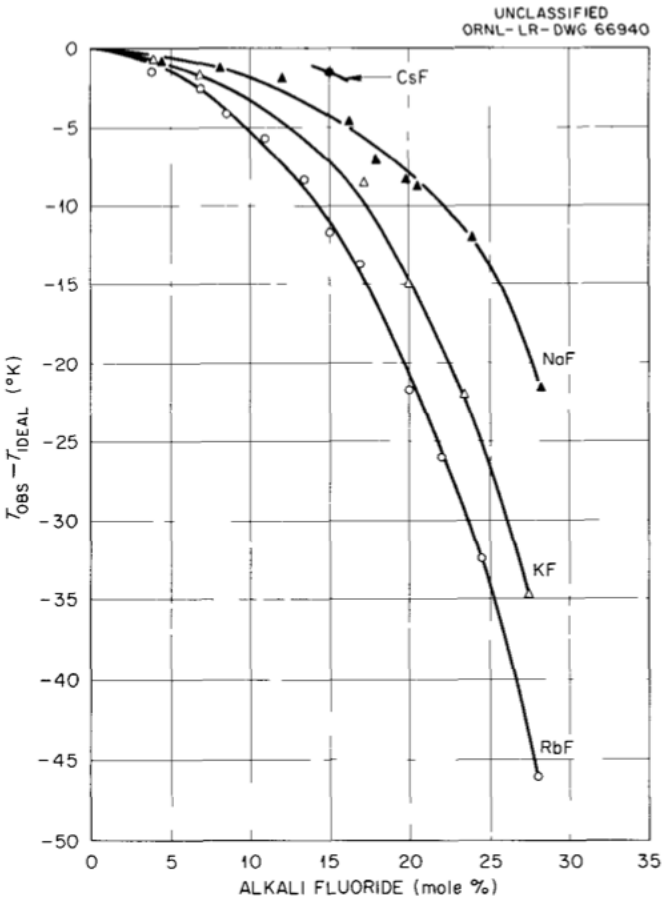

Figure 2-9: Deviation from ideal freezing-point depressions by alkali fluorides in LiF [16]

Blander has provided evidence on the nonnegligible contribution of non-Coulombic interactions (i.e., van der Waals forces) to the heat of mixing for nitrate salt mixtures [18]. Additionally, Bredig would later discuss the effect on excess free energy of mixing for common-cation systems with mixed anions of different size and polarizability [19].

Bredig notes that in common-cation mixed-anion systems, it is not the difference in size that dominates so much as it is the difference in polarizability of the two anions. The large difference in van der Waals-London dispersion forces between F^- and I^- ions dominates the contribution, which results in a positive deviation from ideality for iodine.

He comes to this conclusion by comparing to another system with anions of similar size difference but small polarizability differences.

Later, the partial molar excess free energy of mixing was estimated using activity coefficient data from these freezing-point depression studies with equation 2-25 [14]. The values of $\ln \gamma_{NaF}$ were found from the liquidus temperatures and integration of equation 2-40:

$$R\, d \ln \gamma_i\, x_i = \frac{\Delta H_{fus}}{T^2} dT \qquad \textbf{2-40}$$

where ΔH_{fus} is the heat of fusion of NaF at liquidus temperature T. Results for all the divalent, trivalent, and tetravalent cations were similar, where a negative partial molar excess free energy of mixing was found for NaF in the binary systems. This increasingly more negative free energy can also be interpreted as an increase in stability for NaF in the molten salt mixture, that is, an increasing difficulty to crystallize NaF out of the liquid solution. As alluded to earlier, differences include a reversal in trend in the value of excess free energy as a function of cation size for some of these cations. For example, one would expect AlF_3 to have the most negative excess free energy value as it is the smallest trivalent cation investigated, but the excess free energy of ScF_3 was found to be more negative. Similar to the reversal in trend seen for some of the tetravalent fluorides, such as ZrF_4, this can be interpreted as the Al^{3+} ion not being large enough to permit contact of all six coordinated fluoride ions. This equates to a reduction in the fluoroacidity of the cation. Therefore, NaF is relatively more stable in a solution with a trivalent cation that is slightly larger due to the benefits of sterics.

2.2.2 Molten Salt Solution Models

Estimating the thermodynamic properties of dilute components such as fission products in molten salts can be accomplished using various models of increasing sophistication, typically based on statistical mechanics. Some approaches include: an ideal solution with negligible interactions between particles; a regular solution model with a nonzero enthalpy of mixing; and a subregular solution model which adds non-random entropy of mixing to the regular solution. Because molten salts experience structural ordering around certain compositions, a more sophisticated thermodynamical depiction of the solution was desired.

In 1987, Blander provided a brief history of molten salt thermochemical modeling research that had occurred up until that point [20]. He acknowledges the early experimental work that was carried out at ORNL during the MSR programs, and he notes the importance of a 1954 paper by Flood, Førland, and Grjotheim in establishing early theories on reciprocal molten salt systems [21]. This work would lay the groundwork for many models in molten salt thermochemistry by providing a model which approximated the total excess free energy of mixing of three components in a ternary reciprocal system (a system containing at least two cations and at least two anions) by a handful of terms which are a function of composition and λ_i, the "regular" solution interaction parameters of the binary system of common component *i*.

Although this did not fully explain certain discrepancies in the phase diagram, it led to further developments by Blander and Braunstein who added a term based on a series expansion of equations deduced from the quasichemical theory of solutions (QCT) [22]. The additional term in the model takes into account the coordination number Z of the nearest neighbor ions and was found to be a better predictor of miscibility gaps than the previous model [20], essentially accounting for the effect of non-random mixing. A generalization of the QCT by Blander later led to expressions for the formation of associated, or complex, species in reciprocal systems [23]. Expressions for formation constants of the associated species are a function of Z and specific bond free energy, ΔA, which was later found to be independent of temperature if the associated species is spherical [20]. These models did not fully take into account the theory of Coulomb interactions but provided a good starting point for modeling the activities of multi-component systems based on empirically derived information.

Later, Blander and Saboungi developed an extension to the generalized QCT, leading to the coordination cluster theory (CCT), which applies to dilute solutions of a solute in ionic or metallic solvents [24, 25]. CCT can estimate the correct relative values across a series of compositions (or across a series of similar species) of the specific bond free energies for solutes in reciprocal or additive ternary salt systems. It essentially provides a basis for making predictions of the association energies in these systems. CCT can be used to provide a good estimate of the activity coefficient of an associating solute species in a molten salt solvent given a few assumptions. These assumptions include considering it to be a dilute solute in a binary molten salt solvent forming either an additive or reciprocal ternary system, as well as assuming that the solute does not preferentially solvate in either one of the solvent's components much more so than the other [8].

An example of an additive ternary system would be solute cation S in solvent AX-BX forming (A,B,S//X). An example of a reciprocal ternary system would be solute anion S in solvent AX-BX forming (A,B//X,S). Although it has been shown to provide reasonable results when using approximations for some of the input parameters, it is most accurate when the following parameters are known: (1) the limiting activity coefficients of S in pure AX and in pure BX, (2) the atom fractions of the solvent components, and (3) the activity coefficients of A and B in AX-BX. Although activity coefficient data for some solutes (such as the iodide ion) in the desired pure component solvents may not always be available, CCT has been shown to still provide results of the correct magnitude or correct relative value when comparing to other similar systems [8].

In 1962, Reiss et al. developed the conformal ionic solution theory (CIS) [26]. This statistical-mechanical perturbation theory uses the most fundamental property of a salt: a salt system is a lattice of spherical ions which interact with a spherically symmetric pair potential [20]. The original work only considers hard sphere ions in a binary mixture of two cations with common anion, and the basis of the theory derives from the pair potential of neighboring ions of opposite charge, accounting for the phenomenon described above where it was shown that thermodynamic properties can be approximated as a function of the charge and radii of the interacting ions. The original work on CIS derived an equation for the heat of mixing of a binary system as a function of composition, effective radii, as well as an additional term representing a function of temperature and pressure.

Blander et al. later expanded CIS theory and showed that it was valid for a much more general potential, simplifying higher order terms to show that they are proportional to interionic distances [27] and offering the theory towards reciprocal salt mixtures [28]. He points out that an important conclusion of CIS is that it demonstrates how excess solution properties of ionic systems can be represented as polynomials similar to those used for nonionic mixtures [20]. In the 1970's and beyond, Saboungi and Blander reported much work on molten salt systems at Argonne National Laboratory, further generalizing CIS theory for various applications as well as making predictions a priori [20]. They continued applying CIS to ternary systems including simple reciprocal systems [29], charge-asymmetric reciprocal systems [30], and additive ternary systems [31]. Saboungi further extended CIS theory to higher order systems of ions of the same or different charges in complex multicomponent reciprocal systems [32]. It was shown that solubility products and dilute solute activity coefficients could be calculated a priori because only information on the pure components and binary subsystems are needed in the model. These developments in CIS theory

showed increased sophistication in the types of models, as well as in the types of systems that could be modeled, while still maintaining the ability to predict thermodynamic properties of ternary systems based solely on information from the subsidiary binaries.

Blander notes that ordered solutions, systems often characterized by the formation of complex ions, proved difficult to model with existing theories [20]. An example would be the LiF-BeF_2 system where the formation of BeF_4^{2-} complexes occurs. Such theories might be inadequate for characterizing the thermodynamic properties, which cannot be represented by the use of polynomials for the excess free energies [20]. With this in mind, in 1986, Pelton and Blander developed an empirical extension, or modification, of the QCT for accurately describing the properties of binary silicates as a function of concentration and temperature using only a small number of parameters [33-35]. More importantly, Blander notes that this modified quasichemical model utilizes an empirical combining rule that leads to predictions of the solution properties of multicomponent systems from the subsidiary binaries, and is consistent with the predictions of CIS theory for non-ordered solutions as well as with all available data [20].

2.2.2.1 Modified Quasichemical Model

Developed by Pelton and Blander [33-35], the modified quasichemical model (MQM) for short-range order in liquids in the pair approximation was used in the following decades to estimate the thermodynamic properties of hundreds of oxide, salt, and alloy solutions. In 2000, Pelton et al. published the first in a series of articles summarizing further modifications and extensions of MQM, first covering the application to binary solutions [36]. Later, they applied the updated MQM to multicomponent solutions [37] as well as to systems with two sublattices instead of assuming one [38], which may be a better representation for solutions with very high short-range ordering (SRO). This was further extended with the two sublattice quadruplet approximation (TSQA), to simultaneously take into account the short-range ordering of first-nearest-neighbors (FNN: adjacent cation-anion) between sublattices as well as short-range ordering of second-nearest-neighbors (SNN: adjacent cations or adjacent anions) within the same sublattice. The authors note that this model is perfectly suited to deal with molten ionic solutions due to the model's ability to vary with composition the coordination numbers as well as the ratio of cation-to-anion sites on the sublattices.

The quadruplet approximation refers to the model's ability to account not just for the distribution of pairs, but of quadruplets. In a system of (A,B//X,Y), pairs would include AX, AY, BX, and BY. But for systems where there is a large degree of second-nearest neighbor SRO, the pair approximation does not account for this, and the distribution of quadruplets such as A_2X_2, ABX_2, A_2XY, or ABXY, must be accounted for. This allows for both first- and second-nearest-neighbor SRO to be accounted for simultaneously. The MQM-TSQA accounts for SRO through the use of the second nearest neighbor (SNN) coordination number for each cation and anion in a quadruplet as input parameters. The notation for the SNN coordination number of cation A in quadruplet A_2XY, for example, is $Z^A_{A_2/XY}$. These coordination numbers are semi-empirical model parameters that are not meant to represent the physical coordination number of ions within a melt but should be close to the real values and also must satisfy electroneutrality.

The modified quasichemical model in the two sublattice quadruplet approximation (MQM-TSQA) is an incredibly complex model and therefore the reader is directed to the literature cited above for the derivation and details of the corresponding equations which can represent potential systems. For reference, Chartrand and Pelton have applied it to mixed cation, common halide systems [39, 40] as well as reciprocal multicomponent halide systems [41]. The model can be summarized as being dependent on composition, coordination number, and empirically derived data from the subsidiary systems. The thermodynamic data that is used to represent the lower order systems in the model can include experimental liquidus data, invariant equilibria, enthalpy of mixing values, or activity data. An optimization procedure is utilized to find interaction parameters which fit the model to this experimental thermodynamic data representing the specific pseudobinary or ternary systems, for example. For example, in the case of the quadruplet approximation, this can mean fitting experimental data which represents a binary system of AX-BX to approximate the Gibbs energy change of formation of the quadruplet ABX_2. The benefit of a thermochemical model which only requires information on the lowest order systems (such as binaries) is that a great many different variations of systems can be modeled from just the base information (which can be stored in a database) representing those subsidiary systems and pure components which make up the higher order system. This allows for easy thermochemical modeling of any system via premade computational software, although the accuracy is dependent on the quality and quantity of the binary system data that exists.

A brief introduction to the use of MQM in estimating the solution behavior of molten salts is provided in Section 3. Additional summaries of MQM or other methods which can be utilized in the CALPHAD (Calculation of Phase Diagrams) approach for nuclear fuels such as molten salts can be found in recent literature [4, 42, 43].

2.3 Thermochemical Data Relevant to the KP-FHR

During operation of the KP-FHR, there will be radionuclides dissolved in the Li_2BeF_4 peritectic (FLiBe) coolant salt in various concentrations. Potential sources of radionuclides include fission products escaping TRISO defective fuel particles, impurities, activated corrosion products, and other activation products such as tritium or ^{18}F. In the KP-FHR the vast majority of radionuclides are bound within the TRISO fuel, and as a result, the concentrations of solute impurities that will accumulate in the reactor coolant are expected to be extremely dilute. In the dilute solution limit, solute - solute interactions are anticipated to be negligible. However, it is necessary to conduct appropriate analysis to characterize the chemical system. Through other analyses, the list of relevant radionuclides which need to be considered in the chosen salt system can be found. For the purposes of this study, the relevant elements in dilute concentrations in the FLiBe system that were deemed to be most important in terms of potential volatilization as well as dose toxicity were chosen to be hydrogen (H), cesium (Cs), rubidium (Rb), uranium (U), zirconium (Zr), and iodine (I). Although there are other elements which may be expected to enter the salt, only these elements (which represent a large contribution to the source term) were considered here to showcase the considerable extent to which this system can be modeled.

Provided here is a compilation of the thermochemical data found in literature that is relevant to understanding the behavior of these elements in a molten FLiBe system. Not all of the data here is directly usable by a thermochemical model (such as activity coefficient data that is described in Section 3) but may be indirectly usable through other analyses or in general provide insight on the

behavior of the radionuclides in the coolant salt. Previous work in modeling the thermochemistry of radionuclides in the sodium pool of a liquid sodium-cooled fast reactor provides another example of the importance of experimental data when attempting to model the non-ideality of these complex mixtures [44]. Experimental data relevant to the coolant salt of the KP-FHR is discussed here now. It is emphasized that the concentrations of all solutes in the KP-FHR will be present at very dilute concentrations, less than 0.01 mol%. The solution chemistry discussed in the following sections is mostly obtained from melts containing higher solute concentrations where chemical effects may be exaggerated as solute – solute interactions dominate solution chemistry.

2.3.1 Lithium and Beryllium

A revised phase diagram for the binary system LiF-BeF_2 was published towards the end of the ORNL MSRP [45] although there may be a more updated diagram in current literature for this very common binary salt system (Figure 2-10). The activity coefficients for LiF and for BeF_2 in the FLiBe binary system have been derived from EMF measurements during the MSRP [46] and can be seen graphically below. A power series was assumed for this data and a least-squares fit (combined with Gibbs-Duhem to yield a fit for the other solute) resulted in the following formulas for activity coefficients in the binary system:

$$\log\gamma_{BeF_2} = \left(3.8780 - \frac{2353.5}{T}\right)x_{LiF}^2 + \left(-40.7375 + \frac{36292.8}{T}\right)x_{LiF}^3 + \left(94.3997 - \frac{84870.9}{T}\right)x_{LiF}^4 + \left(-67.4178 + \frac{52923.5}{T}\right)x_{LiF}^5 \quad \textbf{2-41}$$

$$\log\gamma_{LiF} = 0.9384 - \frac{232.08}{T} + \left(-36.9734 + \frac{14652.7}{T}\right)x_{BeF_2}^2 + \left(126.0947 + \frac{74588.5}{T}\right)x_{BeF_2}^3 + \left(-158.4173 - \frac{113592.3}{T}\right)x_{BeF_2}^4 + \left(67.4178 + \frac{52923.5}{T}\right)x_{BeF_2}^5 \quad \textbf{2-42}$$

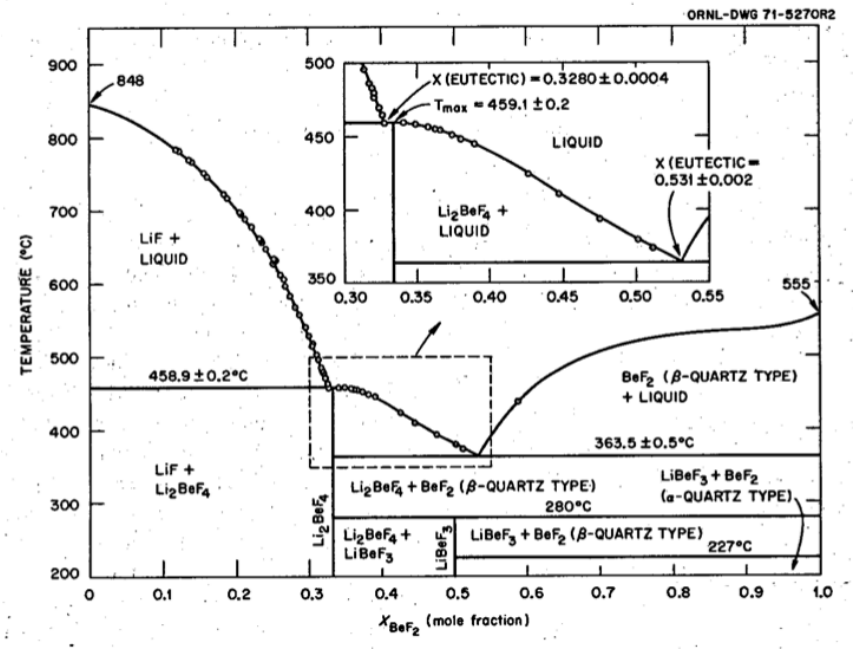

Figure 2-10: Phase diagram for the binary system LiF-BeF_2 [45]

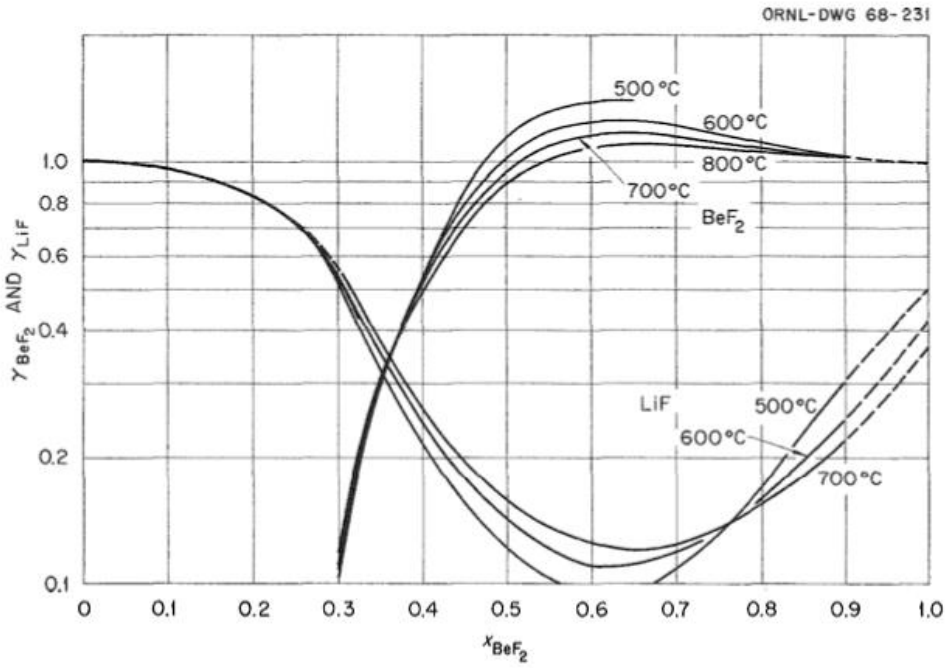

Figure 2-11: Activity coefficients of BeF_2 and LiF in the system LiF-BeF_2 derived from EMF measurements [46]

During the MSRP, experiments were carried out on the evaporative distillation of multicomponent LiF-BeF_2 salt systems [46]. Because of the previous step in the process, distillation was carried out on a system of around 90 mol% LiF and 10 mol% BeF_2, therefore this data is not perfectly applicable to the thermochemistry of the Li_2BeF_4 system due to it having a different effective *Z/r* ratio, as discussed previously. Additionally, the distillation process was carried out at 1000 °C and with concentrations of the third component that are much higher than expected in the KP-FHR. Nonetheless, some conclusions can be made about the relative volatilities of these components and differences can be explained by the differences in the *Z/r* ratio. A summary of the experiment is outlined in Table **2-2**. The seemingly high activity coefficients for RbF and CsF, 2.19 and 1.17 respectively, are attributed to the 90 mol% LiF and 10 mol% BeF_2 solvent melt and are not expected to be representative to the more stable Li_2BeF_4 solvent. Additionally, these values may be within experimental uncertainty ranges from values of unity.

It can be seen that the activity coefficients of UF_4 and ZrF_4 are both well below unity, but the values for RbF and CsF are near or slightly above unity. As mentioned, because the mixture is predominantly LiF, the effective *Z/r* ratio is heavily skewed towards the *Z/r* value for LiF, meaning the addition of any compounds with similar *Z/r* values, i.e., other alkali halides, may not benefit from the negative deviation effects that would otherwise be found in a system with a higher BeF_2 content. Therefore, the thermochemistry of RbF and CsF in these LiF-rich mixtures suggests they will have activity coefficients near unity. It is not clear why a value slightly above unity as opposed to slightly below it was found, although this could be within uncertainty values. Additionally, it could be explained by positive deviation effects that are due to polarizability differences, similar to those described previously for the freezing point deviations found in NaF mixtures, seen in Figure 2-8.

Table 2-2: Apparent partial pressures, relative volatilities, and effective activity coefficients in Li_2BeF_4-metal fluoride systems [46]

Salt Composition (mole %)			Species	Apparent Partial Pressure[a]		Effective Activity Coefficient at 1000°C	Relative Volatility with Respect to LiF at 1000°C
LiF	BeF_2	3d Component		A	B		
86	14		LiF	8.497	11,055	1.60	
			BeF_2	7.983	10,665	4.42×10^{-2}	3.82
90	10		LiF	7.604	10,070	1.30	
			BeF_2	8.707	11,884	3.55×10^{-2}	3.77
95	5		LiF	8.804	11,505	1.30	
			BeF_2	11.510	15,303	4.33×10^{-2}	4.40
90	10	0.02 UF_4	LiF	9.481	12,386	1.33	
			BeF_2	9.339	12,411	5.96×10^{-2}	6.19
			UF_4	4.361	12,481	7.36×10^{-3}	2.9×10^{-2}
89.6	9.9	0.5 UF_4	LiF	8.384	10,987	1.34	
			BeF_2	7.421	10,112	4.65×10^{-2}	4.78
			UF_4	6.686	13,443	1.09×10^{-2}	4.2×10^{-2}
86.4	9.6	4.0 UF_4	LiF	10.790	13,992	1.55	
			BeF_2	10.177	13,726	3.84×10^{-2}	3.42
			UF_4	10.272	16,786	1.25×10^{-2}	4.2×10^{-2}
90	10	0.09 RbF	LiF	8.286	10,811	1.47	
			BeF_2	6.596	10,552	3.11×10^{-2}	2.93
			RbF	5.187	8,907	2.19	24.7
89.9	10	0.03 CsF	LiF	9.654	13,459	1.99	
			BeF_2	8.310	11,313	4.07×10^{-2}	2.82
			CsF	0.819	3,375	1.17	95.1
90	10	0.083 ZrF_4	LiF	7.915	10,358	1.41	
			BeF_2	7.167	10,070	2.83×10^{-2}	2.77
			ZrF_4	13.095	20,382	5.39×10^{-4}	2.19

[a] Log p (mm) = $A - B/T$ (°K). Temperature range: 900 to 1050°C. It was assumed that LiF, BeF_2, and the solute fluorides existed only as monomers in the vapor.

Also during the MSRP, a separate experiment was carried out to better understand the volatility of rare earth fluorides mixed with either LiF or LiF-BeF_2 [47]. They compared the relative volatility (with respect to LiF) of four lanthanide trifluorides (LnF_3, Ln = La, Ce, Pr, Nd) for: the pure LnF_3, the LnF_3 mixed with LiF, and the LnF_3 mixed with a mixture of LiF-BeF_2. Although experimental errors may have been introduced, they found that the relative volatility was reduced by adding BeF_2 to the system for three of the four lanthanides tested. This falls in line with the discussion above on FLiBe mixtures providing effects of negative deviations from ideality. Most of the reported data is shown in Table **2-3**, and shows that these tested lanthanide fluorides, along with YF_3 and BaF_2, are shown to have activity coefficients around unity. These experiments were run with similar LiF compositions as those discussed above for RbF or CsF in 90 mol% LiF, therefore the seemingly higher activity coefficients can be accounted for by the shift in effective Z/r ratio from that expected for FLiBe used in KP-FHR.

Table 2-3: Relative volatilities of rare earth trifluorides, YF_3, BaF_2, SrF_2 at 1000 °C with respect to LiF found with custom molten salt still [47]

Component	Calculated Relative Volatility	Measured Relative Volatility in Ternary System	$\frac{\alpha_{experimental}}{\alpha_{calculated}}$	Relative Volatility in Binary System	$\frac{\alpha_{experimental}}{\alpha_{calculated}}$
NdF_3	3.0×10^{-4}	$<3 \times 10^{-4}$	<1	6×10^{-4}	2.0
CeF_3	2.5×10^{-4}	3.3×10^{-4}	1.32	4.2×10^{-4}	1.68
BaF_2	1.0×10^{-4}	1.1×10^{-4}	0.69		
YF_3	5.9×10^{-4}	3.3×10^{-5}	0.56		
LaF_3	4.1×10^{-5}	1.4×10^{-4}	3.4	3×10^{-4}	7.3
SrF_2	6.8×10^{-6}	5.0×10^{-5}	7.4		

2.3.2 Tritium

Understanding tritium's behavior in molten fluoride salts goes beyond just measuring its solubility in the corresponding salt system. An understanding of the redox potential of the entire salt system and environment is needed to estimate the redox state of tritium (hydrogen cation or elemental hydrogen gas), and thus its chemical and phase distribution. Many computational tritium models have been created and are continuing to be developed for various reactor systems analysis codes, therefore it may be desirable to use these modeling tools to estimate the fraction of tritium in the gaseous or ionic form due to potential coupling with other redox-dependent processes such as corrosion, uranium charge/concentration, etc. A standalone thermochemical model can also estimate this distribution, based on thermodynamic property minimization as discussed previously and in the following section. Discussed here are the relevant data found in literature for the two most common chemical forms of tritium in molten FLiBe: hydrogen gas and hydrogen fluoride.

Recently, Lam et al. used computational methods based on first principles to elucidate tritium chemistry and transport properties in molten fluoride salts [48]. Their results agree with the Henry's coefficient data below in that $^3H^+$ has a higher solubility than $^3H^0$ in FLiBe. They found ionic tritium to be in several chemical forms during the course of the simulation, most commonly as HF, HF_2^-, BeF_4HF^{2-}, and $Be_2F_7HF^{3-}$, where ionic tritium was found as HF around 50% of the time. Interestingly, at least in the temperature range 973-1373 K, between 20-35% of the ionic tritium was found with a coordination number of 2, i.e., as HF_2^-. And over the same temperature range, the fraction of tritium as a free ion was found to increase from around 5% up to 20%. As expected, in both FLiBe and FLiNaK, results indicate that elemental tritium $^3H^0$ shows little chemical interaction with surrounding ions, and that $^3H^0$ can be expected to be in the diatomic form H_2 with weak solvation in fluorine.

2.3.2.1 Gaseous Tritium

Malinauskas and Richardson measured the solubility of hydrogen and deuterium gas in Li_2BeF_4 during the MSRP at ORNL [49, 50]. They did not find a statistically significant "isotope effect" with regards to a difference in solubility between hydrogen and its heavier isotope, deuterium,

therefore it can be assumed that tritium gas (T_2) or tritiated gas (HT) will have a similar solubility: [49]

> *"Also, the data obtained thus far give no substantive indication of a possible isotope effect for solubility; within the limits of mutual uncertainty, the solubilities of hydrogen and deuterium appear to be identical."*

The Ostwald coefficient, K_c, which is the ratio of the gas concentration in solution to its concentration in the gas phase, is displayed in Table for hydrogen, deuterium, and helium in the FLiBe salt at three temperatures. As expected, it can be seen that temperature has a strong effect on solubility, therefore emphasis should be placed on elucidating solubility values of hydrogen gas in prospective molten salts at more temperatures to better understand the behavior. The authors note that Ostwald coefficients are independent of saturation pressure, and it is also not clear the extent to which these values are valid for large volumes of salt, most of which may not be in direct contact with the saturated vapor phase.

Table 2-4: The solubilities of hydrogen, deuterium, and helium in Li_2BeF_4 [50]

T (K)	K_{c,H_2} x 10^3	K_{c,D_2} x 10^3
773	1.13 ± 0.08	1.41 ± 0.08
873	3.17 ± 0.09	2.74 ± 0.16
973	3.87 ± 0.37	4.26 ± 0.44

The Ostwald coefficient can be related to Henry's constant by equation 2-43 [50], but it should be noted that the units of this so-called Henry's constant are different than that defined above in Henry's law in equation 2-27, where that constant is defined as the ratio of the partial pressure of the solute in the gas phase to the solute's liquid mole fraction. The units of this Henry's constant are moles of solute dissolved per mL of melt per atm of saturation pressure of the gaseous solute above the melt.

$$K_c = K_h\, RT \qquad \textbf{2-43}$$

The authors also provide the heat and entropy of solution for the solubility of these gases.

2.3.2.2 Ionic Tritium

The solubilities of hydrogen fluoride (HF) and deuterium fluoride (DF) were measured in Li_2BeF_4 by Field and Shaffer as part of the MSRP in the same temperature and solute saturation pressure range as hydrogen gas above [51-53]. They report the values of Henry's constant, K_h, as units of moles of HF (or DF) dissolved per mol (or mL) of melt per atm of saturation pressure.

Table 2-5: Henry's law constants for the solubilities of hydrogen and deuterium fluoride in Li_2BeF_4 [51]

T (°C)	$K_{h,HF}$ (10^{-4} mol solute/mol of melt-atm)	$K_{h,DF}$ (10^{-4} mol solute/mol of melt-atm)
500	3.37 ± 0.13	2.96 ± 0.07
600	2.16 ± 0.05	1.83 ± 0.03
700	1.51 ± 0.06	1.25 ± 0.03

This form of Henry's law constant can be used by multiplying the value by the saturation pressure of the solute (e.g., TF) above the melt as well as the total moles of melt to arrive at the moles of TF dissolved in the melt.

2.3.3 Cesium

The CsF-BeF_2 binary phase diagram can be found in literature [54] and thermal analysis of the system has been discussed briefly in ANP progress reports [9], although an updated look at this important binary is probably advisable. The binary phase diagram for LiF-CsF can be found in Figure **2-12** and the phase diagram for CsF-ZrF_4 system can be found in Figure **2-23** below.

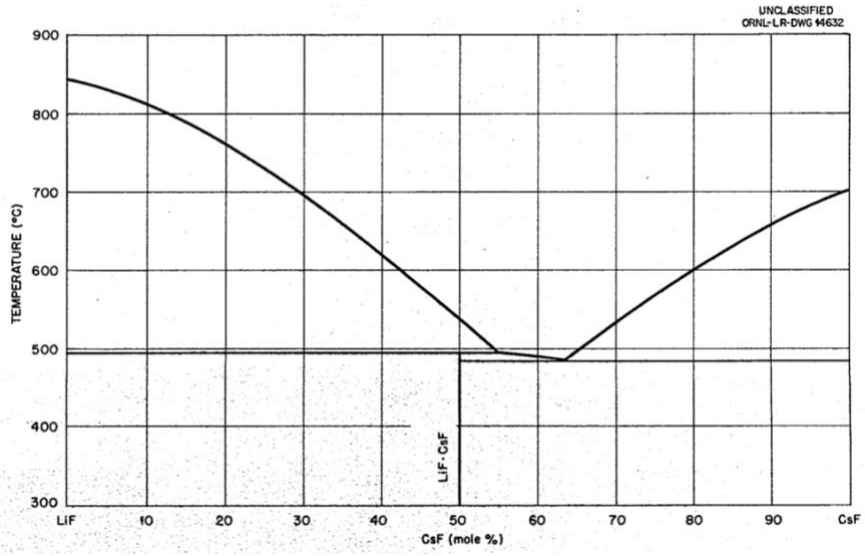

Figure 2-12: Binary phase diagram for the system LiF-CsF [55]

The total vapor pressure of the binary system of CsF and BeF_2 was measured during the MSRP (Figure 2-13). A reduction in vapor pressure is found near the mole ratio of 2:1 alkali:Be, which is similar negative deviation behavior as that seen in other alkali fluoride binaries with BeF_2. Especially noteworthy is that the vapor pressure of the system is always lower than the pure component vapor pressure of CsF, indicating a negative deviation for all concentrations of CsF if mixed with BeF_2, although it is not confirmed if this behavior is consistent at all temperatures above 1000 °C based on the qualitative nature of the figure.

Evidence from the binary system LiF-CsF also supports the belief that CsF will have a negative deviation from ideality in this salt mixture. It has been shown that the LiF-CsF binary system has a negative heat of mixing [56, 57], and further supported by negative heats of mixing also found for other halide binary systems of LiX-CsX (X = Cl^-, Br^-) [58], as well as for the LiF-KF binary [16]. In fact, practically all systems of the form LiX-AX (A = alkali, X = any anion) experience negative enthalpies of mixing [59].

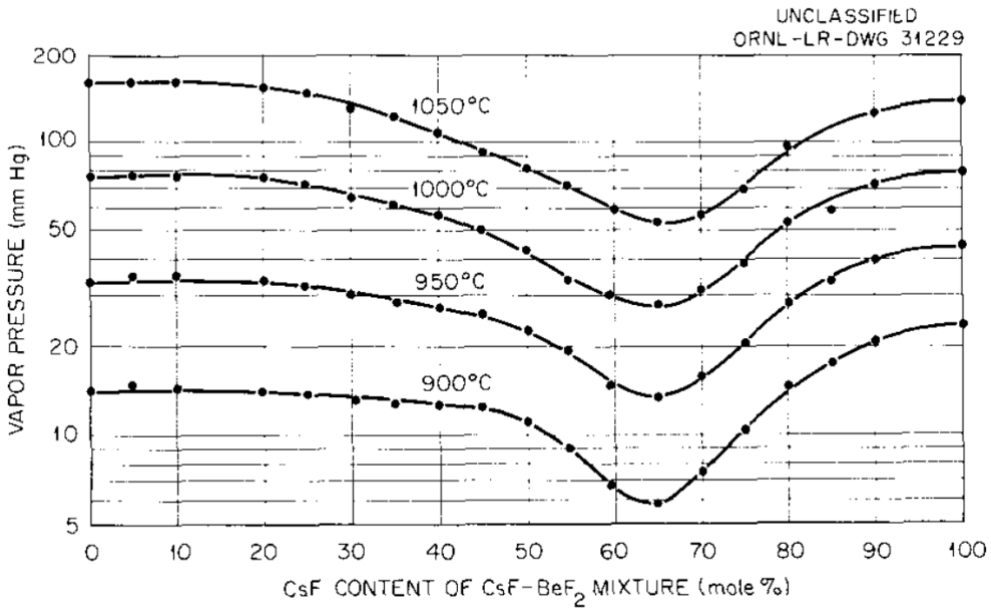

Figure 2-13: Total vapor pressures in the system CsF-BeF_2 [60]

2.3.4 Rubidium

The binary phase diagrams for RbF with LiF and with BeF_2 can be seen below. Based on Figure 2-9, it can also be seen that adding RbF to LiF will decrease the freezing point at all mole fractions tested (<30 mol%), indicating a negative deviation from ideality. Therefore, RbF is expected to have an activity coefficient of $\gamma \leq 1$. This is also supported by the LiF-RbF binary system having a negative heat of mixing [56, 57], and further supported by negative heats of mixing also found for other halide binary systems of LiX-RbX (X = Cl^-, Br^-) [58], as well as for the LiF-KF binary [16].

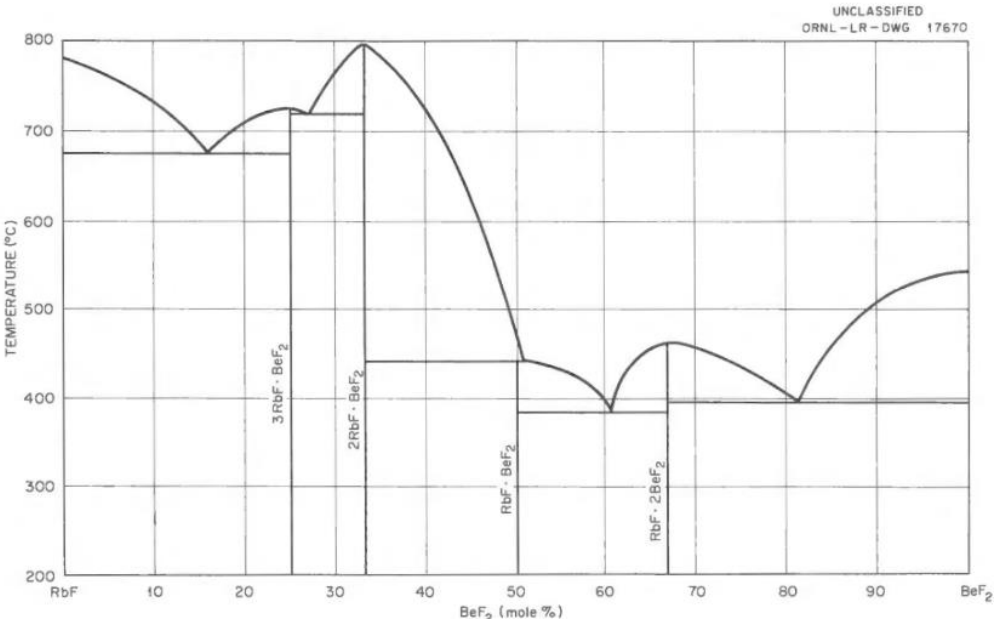

Figure 2-14: Binary phase diagram for the system RbF-BeF_2 [9]

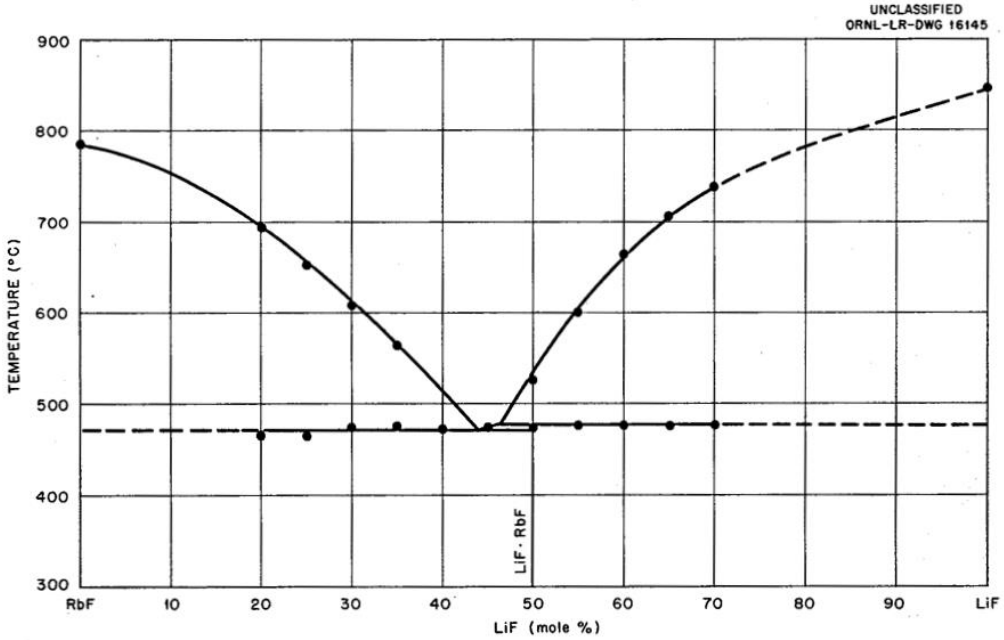

Figure 2-15: Binary phase diagram for the system LiF-RbF [55]

2.3.5 Uranium

The relevant binary phase diagrams for UF_4 mixed with LiF, BeF_2, and CsF, and the binary phase diagram for LiF-UF_3 can be found below, as well as the invariant equilibria for the ternary system LiF-BeF_2-UF_4.

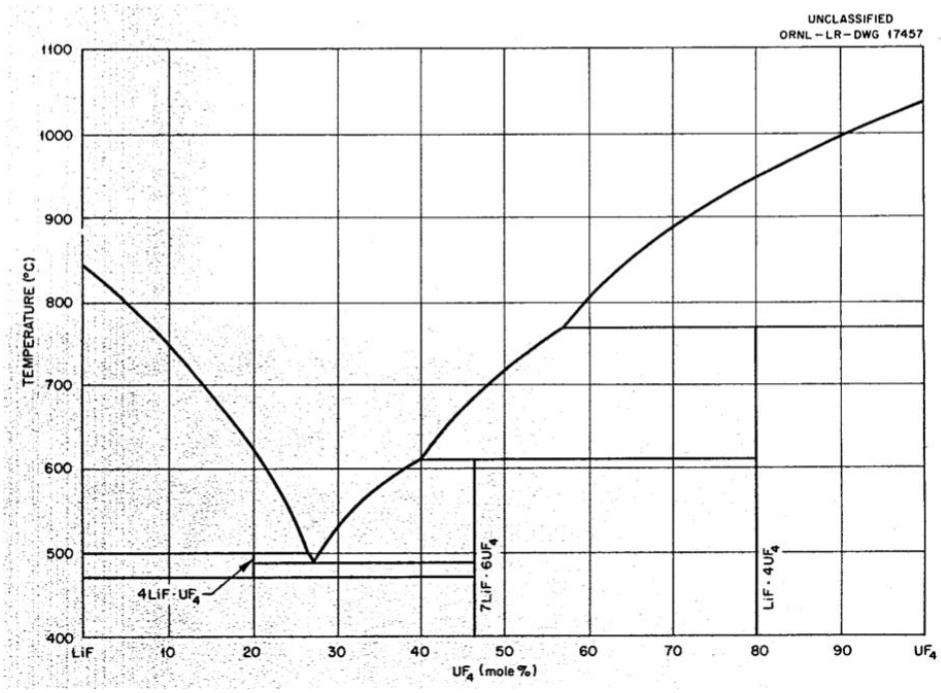

Figure 2-16: Binary phase diagram for the system LiF-UF_4 [55]

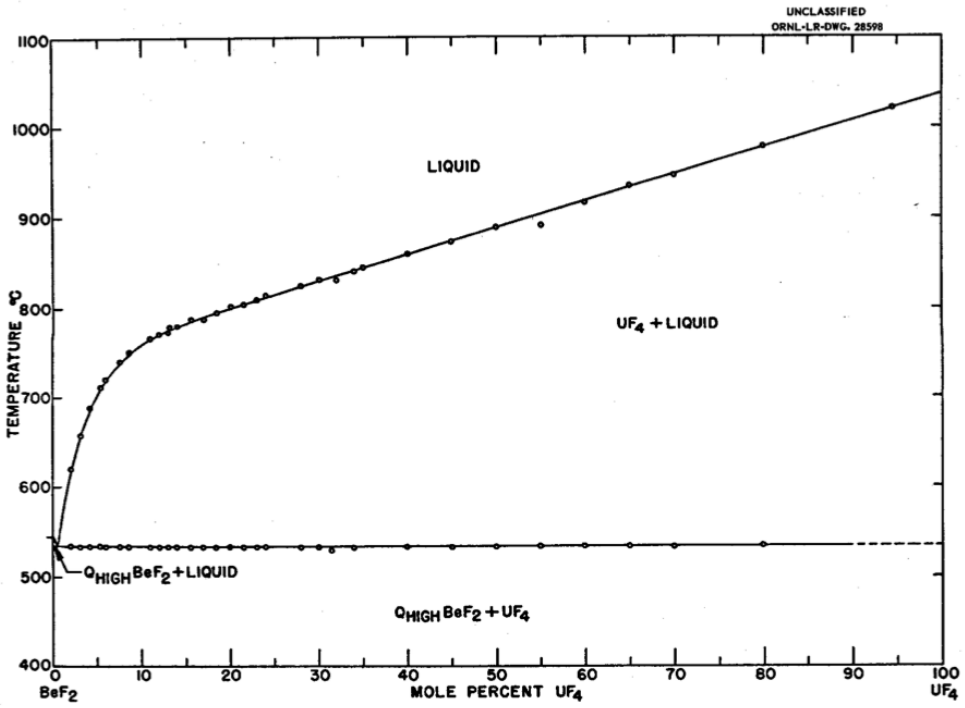

Figure 2-17: Binary phase diagram for the system BeF_2-UF_4 [55]

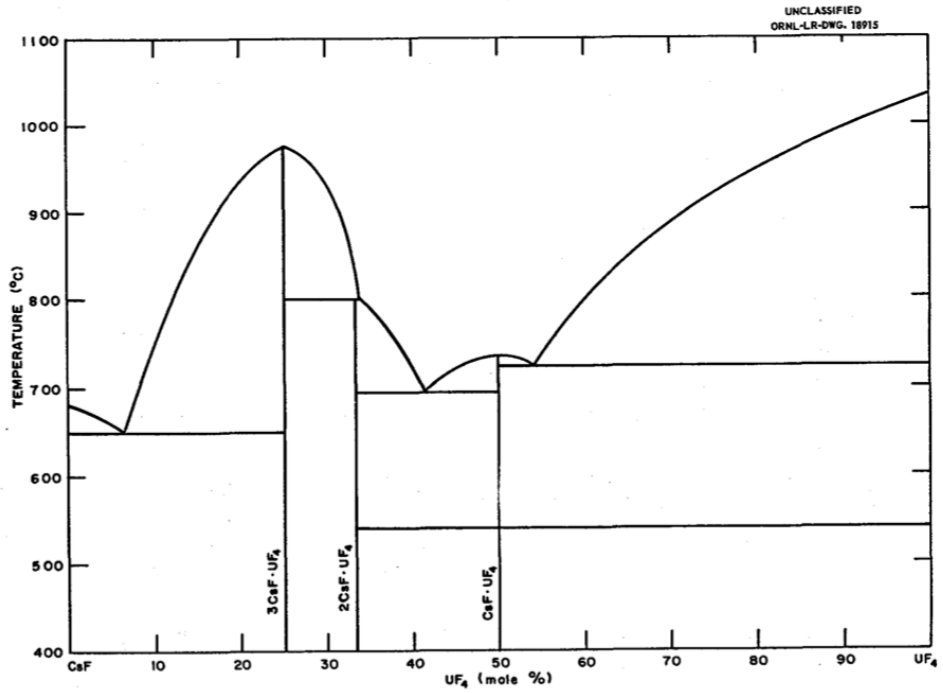

Figure 2-18: Binary phase diagram for the system CsF-UF_4 [55]

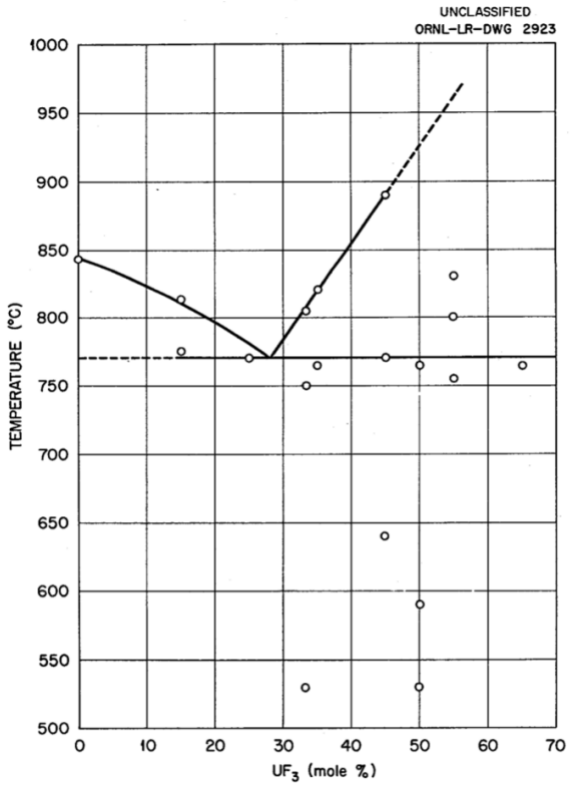

Figure 2-19: Binary phase diagram for the system LiF-UF_3 [55]

Table 2-6: Invariant equilibria in the system LiF-BeF_2-UF_4 [55]

Composition of Liquid (mole %)			Temperature (°C)	Type of Equilibrium	Solid Phases Present at Invariant Temperature
LiF	BeF_2	UF_4			
72	6	22	480	Peritectic (decomposition of $4LiF{\cdot}UF_4$ in the ternary system)	$4LiF{\cdot}UF_4$, LiF, and $7LiF{\cdot}6UF_4$
69	23	8	426	Eutectic	LiF, $2LiF{\cdot}BeF_2$, and $7LiF{\cdot}6UF_4$
48	51.5	0.5	350	Eutectic	$7LiF{\cdot}6UF_4$, $2LiF{\cdot}BeF_2$, and BeF_2
45.5	54	0.5	381	Peritectic	$LiF{\cdot}4UF_4$, $7LiF{\cdot}6UF_4$, and BeF_2
29.5	70	0.5	483	Peritectic	UF_4, $LiF{\cdot}4UF_4$, and BeF_2

As mentioned previously and shown in Table **2-2**, the activity coefficient of UF_4 in a LiF-BeF_2 (90 mol% - 10 mol%) mixture is on the order of 10^{-3} to 10^{-2} at 1000 °C. While adding more BeF_2 to the mixture may increase the effective *Z/r* ratio closer to that of UF_4, the activity coefficient should still be below unity and should not change too much due to benefits of having more associating Be-species in solution and an effective *Z/r* ratio that is still far from that of UF_4.

Uranium tetrafluoride could also be oxidized to the penta- and hexafluoride states if the system is oxidizing enough and provides enough free fluorine to do so. Although this would be a special case scenario and is unlikely to occur during normal operation, the behavior of UF_6 in Li_2BeF_4 must be considered. Unfortunately, there does not appear to be any experimental solubility data for UF_6 in molten fluoride salts without the use of a fluorinating agent like fluorine gas to help separate it out. Therefore, a starting point can be a consideration of the solubilities of HF (as discussed above) or of the bulkier boron trifluoride (BF_3). The solubility of BF_3 was experimentally measured during MSRP in the temperature range 520-725 °C [61]. A least-squares fit of the data yielded a formula for the Henry's law constant as a function of temperature in Kelvin:

$$\ln K_h = -15.076 + 7903/T \qquad \textbf{2-44}$$

The units for the Henry's law constant are mole fraction of BF_3 per atm of saturating pressure of BF_3 above the melt. From this, the solubility of BF_3 appears to be about an order of magnitude larger than that for HF and DF in molten Li_2BeF_4, therefore one might deduce that the thermochemical solubility of UF_6 is probably at least an order of magnitude larger than that for BF_3, given the sterics of the much bulker actinide hexafluoride. BF_3 could provide a minimum bounding value for the solubility of UF_6 if no other data exists.

2.3.6 Zirconium

As shown above in Figure 2-4, the activity coefficient of ZrF_4 in a binary system with LiF was shown to be always below unity, exhibiting a negative deviation from ideality at all concentrations. An updated version of the low concentration region was later reported in a subsequent report (Figure 2-24), also by utilizing equation 2-39 and the liquidus curve method described in the previous section. Additionally, the activity coefficient of ZrF_4 at low mole fractions in Li_2BeF_4 was estimated from chemical reaction equilibria data during MSRP [62].

The invariant equilibria for the ternary system of LiF-BeF_2-ZrF_4 are tabulated below, and the binary phase diagrams for ZrF_4 with BeF_2 and with LiF can be seen below. The binary phase diagram for CsF-ZrF_4 can be found in literature [63] as well as in Figure **2-23** [14].

As mentioned previously and shown in Table **2-2**, the activity coefficient of ZrF_4 in a LiF-BeF_2 (90 mol% - 10 mol%) mixture is on the order of 10^{-4} at 1000 °C. While adding more BeF_2 to the mixture may increase the effective Z/r ratio closer to that of ZrF_4, the activity coefficient should still be below unity and should not change too much due to benefits of having more associating Be-species in solution and an effective Z/r ratio that is still far from that of ZrF_4.

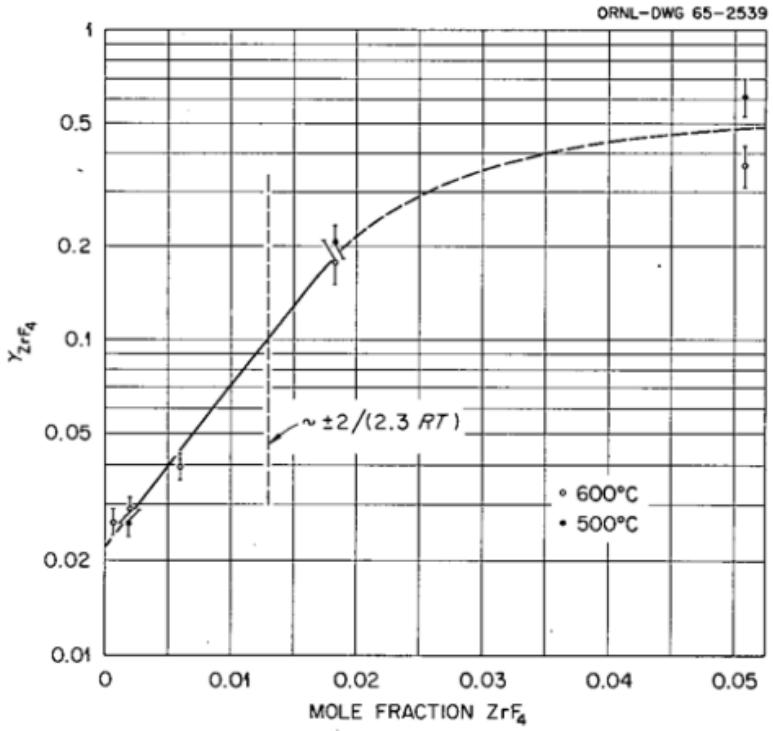

Figure 2-20: Estimated variation of the activity coefficient of ZrF_4 in Li_2BeF_4 melts [62]

Table 2-7: Invariant equilibria in the systems BeF_2-ZrF_4 and LiF-BeF_2-ZrF_4 [64]

Composition (mole %)			Temperature (°C)	Type of Equilibrium	Solid Phases Present
LiF	BeF_2	ZrF_4			
	92.5	7.5	525	Eutectic	BeF_2, ZrF_4
	86	14	645		ZrF_4
	74	26	645		ZrF_4
75	5	20	480	Peritectic	LiF, $3LiF \cdot ZrF_4$, $2LiF \cdot ZrF_4$
73	13	14	470	Peritectic	LiF, $6LiF \cdot BeF_2 \cdot ZrF_4$, $2LiF \cdot ZrF_4$
67	29.5	3.5	445	Peritectic	LiF, $6LiF \cdot BeF_2 \cdot ZrF_4$, $2LiF \cdot BeF_4$
64.5	30.5	5	428	Peritectic	$6LiF \cdot BeF_2 \cdot ZrF_4$, $2LiF \cdot ZrF_4$, $2LiF \cdot BeF_2$
48	50	2	355	Eutectic	$2LiF \cdot ZrF_4$, $2LiF \cdot BeF_2$, BeF_2
47.5	10	42.5	466	Peritectic	$2LiF \cdot ZrF_4$, $3LiF \cdot 4ZrF_4$, ZrF_4
44	18	38	460	Eutectic	$2LiF \cdot ZrF_4$, BeF_2, ZrF_4
27	46	27	532		BeF_2, ZrF_4
2	88	10	532		BeF_2, ZrF_4

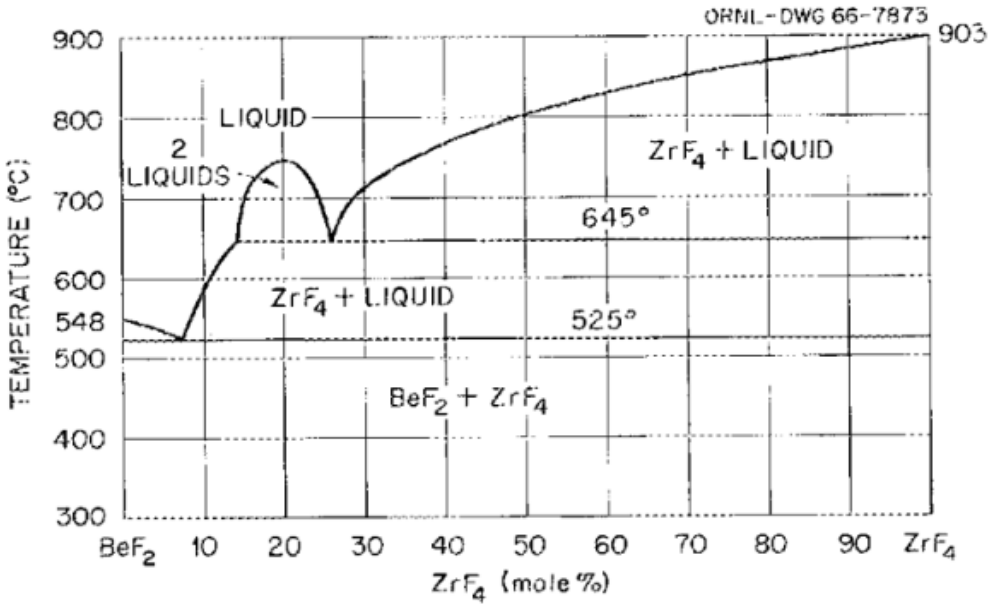

Figure 2-21: Binary phase diagram for the system BeF_2-ZrF_4 [64]

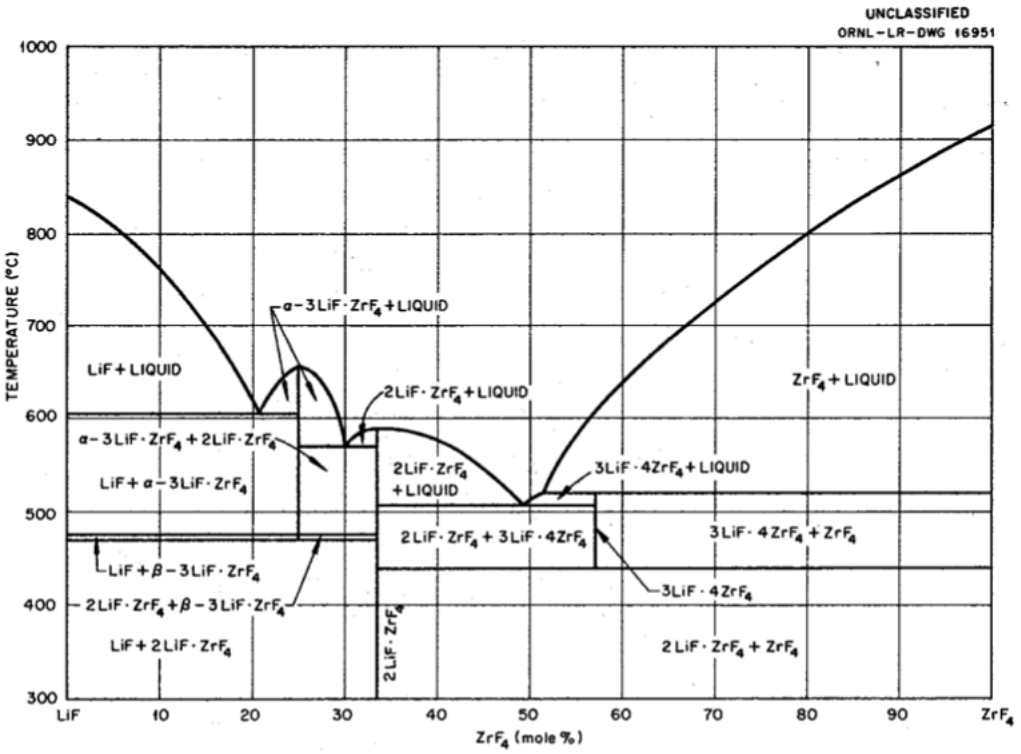

Figure 2-22: Binary phase diagram for the system LiF-ZrF_4 [55]

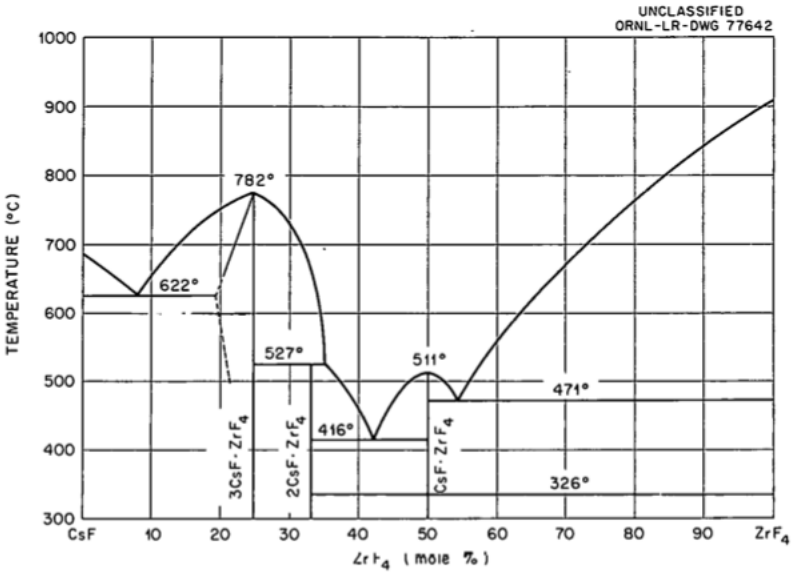

Figure 2-23: Binary phase diagram for the system CsF-ZrF_4 [14]

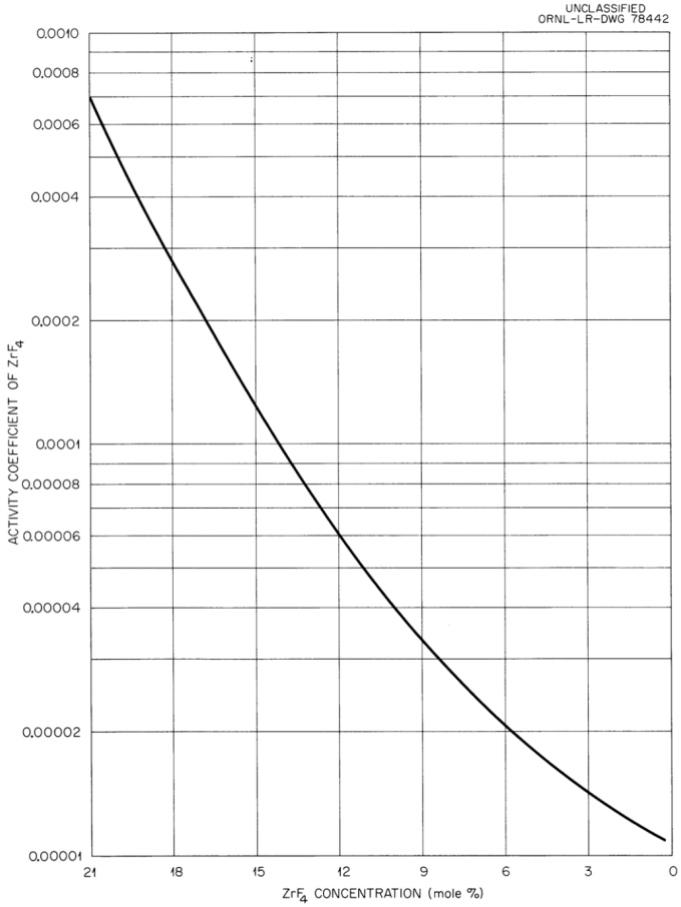

Figure 2-24: Activity coefficients of ZrF_4 in the system LiF-ZrF_4 in the low concentration range [65]

2.3.7 Iodine

Melnichak and Kleppa experimentally measured negative enthalpies of mixing for all binary systems of mixed alkali cations with common iodide ion [66]. Values are the most negative (most stabilizing) for the systems with cations of the greatest difference in size such as LiI-CsI. Sekiguchi et al. later confirmed with molecular dynamics simulations the negative values and the general shape of the curve of the enthalpy of mixing for the LiI-CsI system [67]. Unfortunately, this doesn't say anything about the enthalpy of mixing of a reciprocal system such as LiF-CsI or LiI-CsF because these have more factors in trying to estimate the interaction potential.

Later, Melnichak and Kleppa measured the enthalpy of mixing for binary systems of mixed anions (X=Cl, Br, I) with common alkali metals, and surprisingly a positive enthalpy of mixing was found for all systems [68]. Although they did not include the fluoride ion in any systems, something can be deduced from the trend of the systems tested. For all cations tested, the Cl-I binaries had the largest enthalpy of mixing, followed by Br-I, and then Cl-Br. If the increasing enthalpy of mixing is due to the increasing difference in ionic radii of the anion, then it can be assumed that the Fl-I binary systems will have enthalpy of mixing values even larger (i.e., more positive) than these, for the same cation. The true dependence probably also has to do with differences in polarizability, electronegativity, and/or charge, therefore this should not be viewed as conclusive. Additionally, this does not say anything about the entropy effects of the mixed anion system. Nonetheless, one might expect a positive deviation from ideality (for the iodide compound) if a metal iodide is added to a mixture of metal fluorides.

Melnichak and Kleppa try to explain this positive enthalpy of mixing that is found for the mixed anion systems [68]. They consider the interactions between the second-nearest neighbors to try to rationalize the thermodynamic behavior, noting that there are two main contributions to the enthalpy of mixing. First, the negative contribution which is caused principally by the reduction in the Coulomb repulsive energy between second-nearest neighbor ions, and second, the positive contribution which is attributed mainly to the van der Waals-London interaction between the same ions. They note that the negative contribution is much larger for many mixed cation systems due to the wide variation in ionic sizes between the two different cations. In mixed anion systems, the ionic size differences between the mixed anions are not so large that they contribute a strong enough negative contribution, allowing the positive contribution to dominate.

In support of the ORNL MSRP, Bredig investigated the thermodynamics of common cation-mixed anion systems [19]. Specifically, he looked at the excess free energies of binary systems of common cations (M=Li, Na, Ca) in mixed fluoride-iodide mixtures. He compared the experimentally derived liquidus curves with the Temkin-ideal liquidus computed from:

$$\ln a_i = \frac{\Delta H_{fus}}{R}\left(\frac{1}{T_m} - \frac{1}{T}\right) + \frac{\Delta C_p}{RT}(T_m - T) - \frac{\Delta C_p}{R}\ln\left({}^{T_m}/_{T}\right) \qquad \textbf{2-45}$$

Bredig found positive deviations from ideality (positive excess free energy of mixing) for the LiF-LiI and NaF-NaI systems over the compositions measured yet he does not provide the exact values. He only provides experimental liquidus data points scattered over the entire composition range and displays them relative to an ideal (Temkin) calculation. Although there are no data points at mole fractions below 10 mol% metal iodide, the increase in liquidus occurs at all

concentrations, but it is less pronounced (i.e., closer to ideality) at lower metal iodide concentrations. He also does the same for the divalent system CaF_2-CaI_2, yet the experimental data here does not include the lower composition range of CaI_2, so the liquidus curve is extrapolated. The comparisons of the experimental and ideal liquidus curves are found in Figure 2-25. While a positive excess free energy is found for the divalent system as well, it is smaller (less positive) than that found for the monovalent cation systems. He notes the overall positive excess free energy is due to the large difference in polarizability and its effect on van der Waals interactions between the two anions. But when the iodide ion is in low concentrations, i.e., for fluoride-rich melts, a negative contribution may arise for divalent cations bonded with one of each anion: [19]

> *"However, in fluoride-rich melts a negative component, apparently not previously recognized, may arise from the enhancement in the polarization of I^- by Ca^{2+} in cation-anion-anion configurations, such as $Ca^{2+}I^-F^-$, over that in $Ca^{2+}I^-I^-$ of pure CaI_2. The greater fuel strength of F^-, z/r = -0.73, compared with I^-, z/r = -0.46, leads to an enhancement of the field gradient that the I- in $Ca^{2+}I^-F^-$ encounters."*

Bredig hypothesizes that the higher field strength of the divalent cation and greater anion:cation ratio, which results in greater frequency of MIF configurations, allows for a smaller positive excess free energy for the divalent systems at lower iodide concentrations than that for the monovalent systems [19]. It is noted in Figure 2-25 that the deviation from ideality decreases as the concentration of iodine decreases, becoming negligible in the dilute solution regime. Nonetheless, this still supports the notion that a positive deviation from ideality is to be expected for iodide-bearing compounds when present in high concentrations in molten fluoride salts.

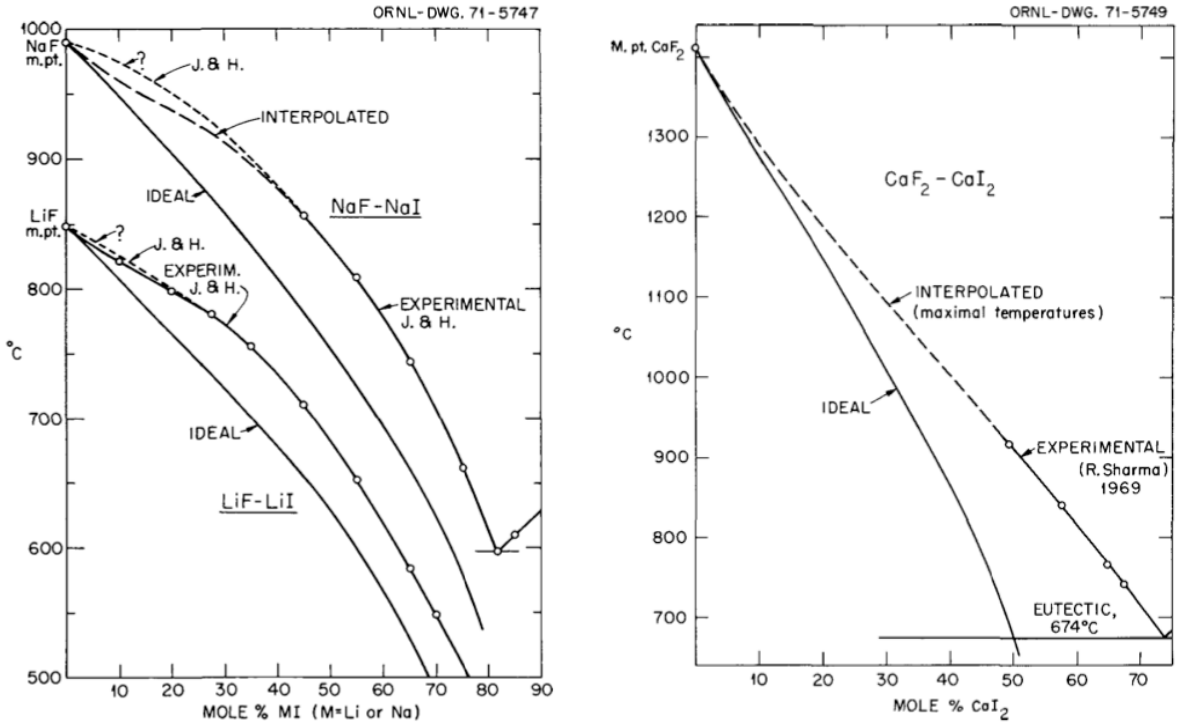

Figure 2-25: Experimental and Temkin-ideal liquidus curves in the systems LiF-LiI, NaF-NaI (left) and CaF_2-CaI_2 (right) [19]

Margheritis et al. mixed LiF with various alkali halides, including CsI, in search of miscibility gaps in these mixtures [69]. Phase diagrams were found for all the pseudobinary systems of the form LiF-AX (A=Na, K, Rb, Cs and X=Cl, Br, I). The LiF-CsI system contained the widest miscibility gap of all systems, extending from near x_{LiF} = 0.01 to almost pure LiF. A miscibility gap is an indication of a maximum in Gibbs energy of the system, representing a point at which the mixture exists as two or more phases. Recently, Sekiguchi et al. confirmed with molecular dynamics simulations the positive values of enthalpy of mixing for the systems LiF-LiI and CsF-CsI at low concentrations of the iodide [67]. They also calculated the enthalpy and excess Gibbs energy of mixing for the reciprocal system LiF-CsI and found positive values for both.
This is further evidence that cesium iodide, and potentially all iodide-containing compounds, will probably have positive deviations from ideality in molten lithium fluoride salt mixtures, although this does not say anything about the effects of being mixed with BeF_2. Additionally, it is currently unknown if these effects are applicable to the KP-FHR where the dilute concentrations of Cs and I may preclude the formation of molecular CsI.

Taira et al. measured the partial pressures of CsI mixed in FLiNaK molten salt [70]. They showed variations in vapor pressure for CsI with different concentrations, but a direct dependency and a general correlation were not clarified. Sekiguchi et al. later clarified the vaporization behavior of CsI above FLiNaK and provided results when varying the ratio of Cs:I to better simulate a nuclear reactor fuel salt, where Cs can be in higher concentration by over an order of magnitude [71]. An increase in the vapor pressure was found when CsI and CsF were added to the salt. Strongly positive deviation was found for CsI, with activity coefficients in the range of 6 to 13, while CsF displayed nearly ideal behavior, with an activity coefficient near unity. The behavior of CsF in this salt is expected, given the high fluoroacidity of FLiNaK when compared to FLiBe. FLiBe should provide a more stabilizing behavior for solute cation fluorides, providing an activity coefficient below unity and a negative deviation from ideality. Capelli et al. studied the thermochemistry of cesium and iodine in the more representative salt solution, $LiF\text{-}ThF_4$ [72]. They used thermodynamic modeling, similar to what will be discussed in Section 3.2, based on experimental data for binary and ternary systems to estimate the vapor-liquid equilibria for this system. They found that when iodine was included in the system, the vapor pressure was much higher, resulting in vaporization of the species CsI out of the system $LiF\text{-}ThF_4\text{-}CsF\text{-}CsI$. They do not provide activity coefficient data but conclude that if cesium is bonded to iodide in the salt, it can be expected to have limited solubility and should be expected to be volatile, noting CsI was the dominant vapor species found. This study does not confirm nor deny the extent to which LiI is formed or vaporizes.

Dworkin and Bredig measured the phase diagrams of the Li_2BeF_4-KI reciprocal pseudobinary system, and similar to that for LiF-CsI, found a large miscibility gap covering most compositions above 5 mol% KI [73]. They found the phase diagram for the Li_2BeF_4-LiI pseudobinary system [61], and later compared it to the same type of system but with Na and Cs ions substituted for Li [45]. These three liquidus (solid) curves are seen below, where the dashed lines represent the ideal liquidus calculated for solute particles that are not dissociated (the “n=5” dashed line represents a special ideal case where the BeF_4^{2-} molecule dissociates to one Be^{2+} ion and four F^- ions). They find that all the systems experience positive deviations from ideality for most compositions greater than around 20 mol% M_2BeF_4, represented by positive values of excess partial free energy of mixing. Although, the experimental and ideal liquidus curves do appear to approach below 10 mol% MI, therefore at concentrations relevant to FHRs or even MSRs, it may

be likely that MI exhibits nearly ideal behavior when mixed with FLiBe. They do not come to a conclusion as to why systems with mixed anions experience these positive deviations, as the interaction potentials are determined by a complicated mix of positive contributions from Coulomb and van der Waals energies, and negative contributions from repulsion and polarization energies. They correctly point out that any previous discussion on effects on enthalpy of mixing only tell half the story on deviations from ideality: [45]

> *"However, we must also remember that the differences reflected in the phase diagrams are due to partial excess free energy of mixing and not necessarily to the enthalpy of mixing, which determines the interaction potential. The explanation for differences in degree of nonideality must then include differences in the entropy of mixing for which little data exists for these systems."*

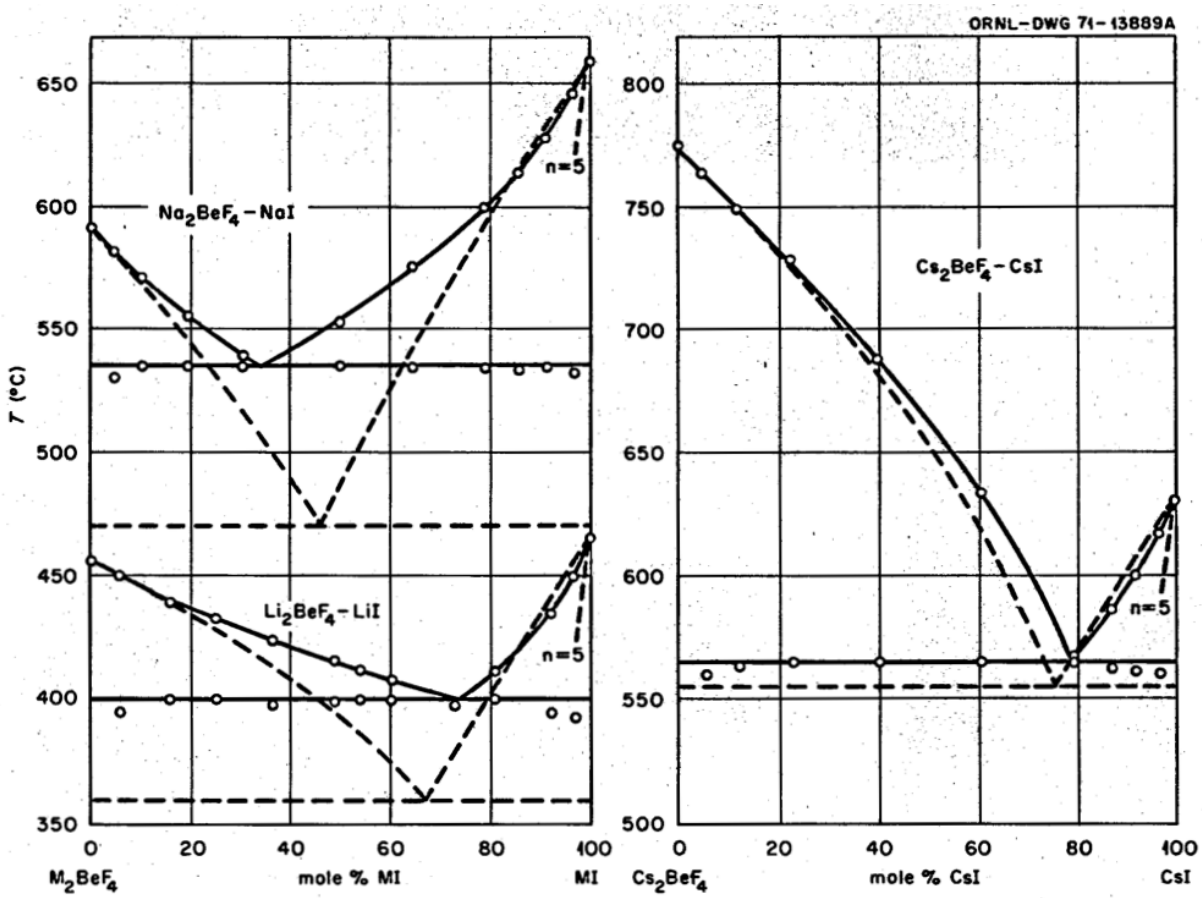

Figure 2-26: Phase diagram for the pseudobinary systems M_2BeF_4-MI (M=Li, Na, Cs) [45]

Further evidence for positive deviations from ideality for common (or mixed) cation systems with mixed anions can be found from investigations of fluoroborate-fluoride binary systems during MSRP. They estimated the activity coefficients of components in the $NaBF_4$-NaF system, the excess chemical potential of NaF in the KBF_4-NaF system, and the liquidus curves compared to ideal curves for the KBF_4-MF (M=Na, K) systems [46, 74]. The activity coefficients were estimated using vapor pressure data and the excess chemical potential data were found from calculations utilizing heat of fusion, heat capacity, and experimental liquidus curve data. They also compared the interaction parameters for excess free energy between two types of mixed

anion systems with the same common cation (Na or K) [74]. They compared the mixed fluoride-fluoroborate system with the mixed fluoride-iodide system and found that smaller cations resulted in less negative deviations from ideality, providing the conclusion that it is the changes in anion packing that cause the positive deviations from ideality: [74]

> *"In both the BF_4^--F^- and I^--F^- systems, deviations from ideality become less negative with decreasing size of the common cation, as would be expected if changes in anion packing contribute positive deviations."*

All of this data bolsters the belief that non-fluoride anions which are added to fluoride-rich salt systems are expected to experience positive deviations from ideality, if any, and should not be credited as having improved retention in the salt compared to their pure component volatility, i.e., a negative deviation from Raoult's law should not be assumed.

2.3.7.1 Iodine Speciation and Volatility

It has been established that the thermochemistry of iodine will probably experience a positive deviation from ideality in molten fluoride salts. But this does not necessarily mean that iodine will completely volatilize from the salt. The first question to be asked is concerned with the speciation of iodine, i.e., if iodine will be in the chemical form of LiI, CsI, HI or something else. Secondly, these species may not necessarily be volatile in the salt system, despite probably having an activity coefficient greater than 1. The positive deviation from ideality only tells us that the dissolved iodide compound (e.g., LiI) will be more volatile than the pure component would be by itself when not dissolved in a solution of fluoride salts. The volatility can be quantified from the pure component vapor pressure and liquid mole fraction, i.e., Raoult's law (equation 2-33). If the compound behaved ideally, $\gamma_A^R = 1$. But if there is a positive deviation from ideality, $\gamma_A^R > 1$. This amounts to a larger than expected partial vapor pressure of the compound than would be calculated if it was not dissolved in the solution.

But even with a positive deviation, the magnitude of the deviation is also important information. Work by Kleppa and collaborators (discussed above) on common cation-mixed anion binary systems have generally shown that the enthalpies of mixing are small, corresponding often to very small excess free energies which produce relatively small deviations from ideality, if any [75].

There is little to no experimental data on dissolving such small concentrations of iodine in molten salts that would be representative to the KP-FHR. At high enough concentrations of each ion, CsI may be assumed to be formed due to a concept known as the "reciprocal Coulomb effect" [69], where in reciprocal salt systems, the two larger ions (e.g. Cs^+ and I^-) bond with each other while the two smaller ions (e.g. Li^+ and F^-) do the same. This is represented in two dimensions in Figure **2-27**. But given the very small concentrations of both Cs and I in the KP-FHR coolant salt, and the fact that molten salts are relatively structured and do not experience random mixing [76], it may not be advisable to assume that all the iodine in the salt will be in the form of CsI. Most may be dissolved in the salt as LiI, or if there is a high enough concentration of hydrogen (or tritium), it may be volatilized as HI (or TI).

Appreciable volatilization of iodine was not found during the Aircraft Reactor Experiment, and although it was speculated that elemental iodine could be reduced to iodide (depending on the

redox conditions and existence of reducing species such as U^{3+}), the formation of "probably BeI_2 or BeIF" species were not considered to be especially volatile [16]. The removal of iodide from fuel salts using HF-H_2 gas mixtures was studied multiple times throughout the MSRP [52, 77, 78]. It was found that iodine can be easily volatilized by sparging hydrogen fluoride-hydrogen gas mixtures. Specifically, "high temperatures and low hydrogen pressures favor the formation of atomic iodine, while HI is formed at high temperatures and relatively higher hydrogen pressures" [77]. Although this may not be representative of an KP-FHR, the experiments provide some understanding on the transport of iodine through the system, most likely in the form of HI [52], or to a lesser extent, atomic or molecular iodine: [77]

> *"The iodine removal mechanism is explained by a model that assumes that the rate-controlling step is the transport of I^- from the bulk of the melt to the surface, and that the rates of the other steps are rapid."*

If it is possible to estimate the production and mass transport rate of tritium fluoride in an FP-FHR (moles TF/hr), it may be possible to estimate iodide removal rates from an KP-FHR coolant salt given the iodine liquid mole fraction [52].

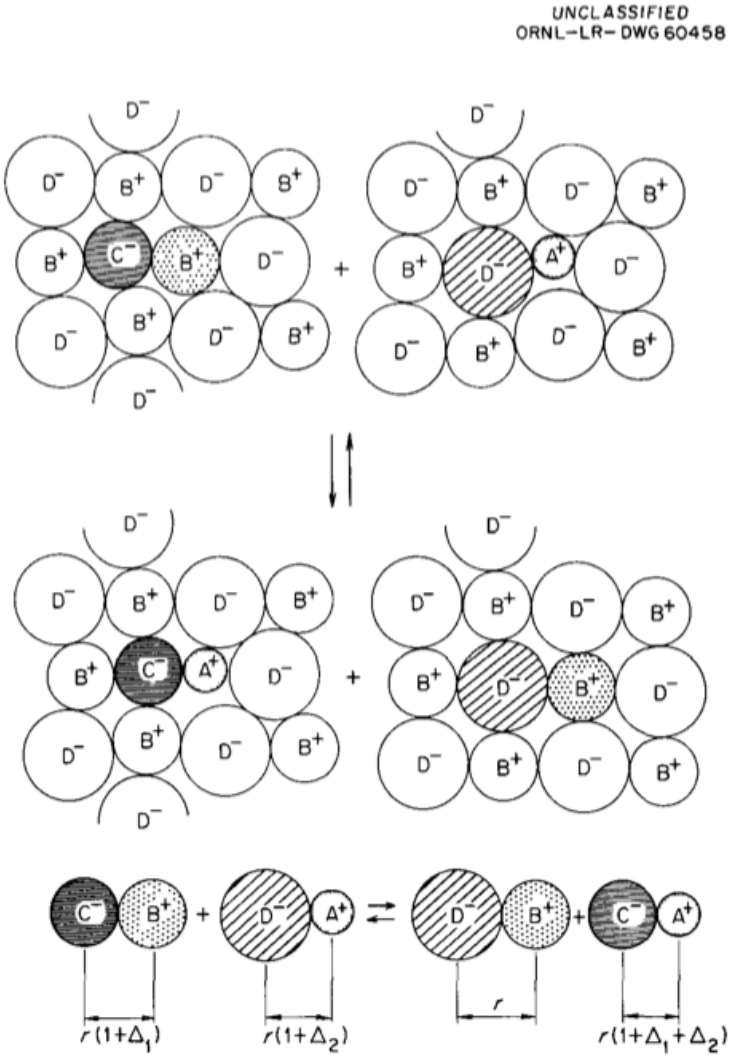

Figure 2-27: Two-dimensional representation of the Reciprocal Coulomb Effect [16]

3 Methodology

Chemical speciation and the determination of phase equilibria in molten salts can be accomplished by combining Gibbs free energy minimization methods with the Calculation of Phase Diagrams (CALPHAD) method [79]. While some chemical systems can often utilize Gibbs free energy minimization methods successfully without the need for sophisticated solution models, molten salts display a certain level of structural ordering, as mentioned in the previous section. The non-ideal effects of fused salt mixtures, largely due to Coulomb interactions, makes accurate thermochemical modeling of molten salts more challenging. Because of this, the estimation of Gibbs free energies of molten salt solutions with more than one end-member (i.e., pure component) requires the use of solution models to properly calculate phase diagram data for the mixture.

In the previous section, the modified quasichemical model (MQM) with two-sublattice quadruplet approximation (TSQA) was introduced as the preferred method of estimating liquid salt solution behavior. MQM-TSQA utilizes interaction parameters which represent the interactions between the four components that make up a representative quadruplet of nearest neighbors in liquid solution (e.g., Li,Be//F,F). For pseudo-binary or higher systems, these interaction parameters are used to represent the effects of the excess Gibbs energy of mixing. It is the implementation of these excess energy functions in the model that accounts for the effects of non-ideality in solution. Therefore, it is necessary to build a thermodynamic database which includes not just the pure component end-members, but also the interaction parameters for each quadruplet. It has been shown that the development of such a thermodynamic database is necessary to efficiently design and analyze molten salts for nuclear applications [43].

3.1 Thermodynamic Modeling Tools for Source Term Modeling

Many chemistry softwares exist to measure chemical and phase equilibria based on pure component thermodynamic properties such as the enthalpy of formation, entropy, and heat capacity. As mentioned, molten salts require an understanding of the excess Gibbs energy of mixing which is often difficult to find. In the previous section, it was shown that this is directly related to activity coefficient data, which is unfortunately also nonexistent for many systems and mixtures. An alternative is to use solution models to model excess thermodynamic properties. These solution models, such as MQM-TSQA, are used in the CALPHAD approach to produce phase diagrams and Gibbs energy equations which represent the mixture. The Gibbs energies of the components which factor in mixing effects can be minimized (given the system conditions) to estimate the chemical form and phase of the radionuclide of interest in the molten salt solution.

Although many chemistry softwares exist, only a few have been developed specifically with MQM in mind. FactSage [80] is one such commercial software which was created in part by the original developers of MQM and has a Gibbs minimization module. Additionally, Thermochimica [81, 82] is an open source Gibbs minimization solver which utilizes MQM but relies on a pre-made thermodynamic database as input, and was developed specifically for nuclear applications such as modeling the thermodynamic behavior of fission products and actinides in solid nuclear fuels [2].

The Nuclear Energy Advanced Modeling and Simulation (NEAMS) program, funded by the U.S. Department of Energy, Office of Nuclear Energy, has supported the development of a Molten Salt Thermodynamic Database (MSTDB) [42, 83]. This includes both thermochemical and thermophysical properties of molten salts. The thermochemical portion, MSTDB-TC, is soon to be released and has been under development for several years [84]. MSTDB-TC is a consistent set of thermodynamic functions for all solids, liquids, and gases of the constituents considered. It is essentially a set of Gibbs energy functions for stoichiometric compounds, solid solutions, liquid solutions, and vapors. It does not contain a Gibbs energy minimizer, therefore, to calculate equilibrium states it should be used with codes like Thermochimica or FactSage, which it has been formatted to work in.

Internationally, a molten salt thermodynamic database utilizing the FactSage software is also being developed by the Joint Research Centre (JRC) in Europe [85].

The FactSage software will be used here to provide an overview of the methodology utilized in developing a thermodynamic database for the molten fluoride salt system of interest to KP-FHR. Unfortunately, the results of this database (speciation results, excess Gibbs energy functions, complex phase diagram data, etc.) will not be shared here due to proprietary information (e.g., the composition of radionuclides in the coolant salt) and due to ongoing refinement of the energy functions. Nonetheless, the process carried out in building this database, which is based on publicly available thermodynamic data and the FactSage software, is provided here and can be found elsewhere in literature [72].

Finally, FactSage can provide speciation results by using the built-in Equilib module and using the aforementioned custom thermodynamic database of non-ideal molten salt solutions, or that provided by MSTDB-TC. Additionally, Thermochimica can provide phase equilibrium calculations based on database files built within FactSage or those from MSTDB-TC. In any case, these vapor and liquid phase speciation results can be used with the pure component vapor pressures to solve for the activity coefficient of that component in the mixture at those system conditions (temperature, pressure, etc.). Activity coefficients are a function of temperature and radionuclide composition and can be estimated with these tools. Such formulas can be used in evaporation models that represent the molten salt pool inside the reactor vessel, or even outside the system in the event of a spill. The activity coefficient describes the deviation from ideal vaporization for that radionuclide (Raoult's Law), and thus can be used to estimate the amount vaporized. The amount of each radionuclide in the vapor phase is necessary information for mechanistic source term models. This is typically tracked throughout various parts of the reactor system, containment vessel, and reactor building assuming leak rates based on structural component failures or building leak rates. Atmospheric dispersion and dose consequence modeling codes can then be used to take the radionuclide beyond the reactor building.

3.2 FactSage

FactSage was used to build a thermochemical model of the 9-element system described previously, consisting of the following elements, with uranium as either the tri- or tetravalent: Li^{+}, Be^{2+}, Cs^{+}, U^{3+}, U^{4+}, Rb^{+}, Zr^{4+}, H^{+}, F^{-}, and I^{-}. It should be noted that all of the compounds containing hydrogen are modeled as ideal, as most are gases at these temperatures, and no fluoride salt solution thermodynamic data was found for those that aren't gases. The methodology

for utilizing FactSage to optimize and calculate phase diagrams for binary, ternary, and more complex systems has been discussed in literature [43] and in FactSage documentation, but will be summarized briefly here. FactSage provides the vapor, liquid, and solid phase mole fraction and activity of each compound expected to be present in a system (i.e., the speciation). The mole fractions of the liquid phase species and knowledge of the pure component equilibrium vapor pressures can be used to calculate the activity coefficients of these species based on Raoult's law (equation 2-33). Calculating these activity coefficients for various compositions and temperatures for the same radionuclide can result in formulas for the activity coefficients as a function of composition and temperature.

FactSage contains several solution models which can be utilized to model the liquid salt solution. A brief overview of FactSage's utilization of thermodynamic data to implement MQM is presented here as a reference.

3.2.1 Pure Compounds

The thermodynamic properties of the pure compounds that were used in the calculation of binary and ternary phase diagrams were taken from references listed in Table 3-1. Alternatively, the thermodynamic data of all pure compounds can be obtained from the built-in database, FactPS. It should be noted that the excess energy parameters discussed in Section 3.2.2 are optimized to be used with a specific set of corresponding end-member thermodynamic values, and so if slightly different values are used, there may be differences in the results. It is recommended that a solution model only use the excess energy parameters that were determined for specific enthalpy, entropy, and heat capacity values.

The Gibbs energy for pure compounds is defined as: [43]

$$G(T) = \Delta_f H^0(298) - S^0(298)T + \int_{298}^{T} C_p(T)dT - T\int_{298}^{T}\left(\frac{C_p(T)}{T}\right)dT \qquad \textbf{3-1}$$

where $\Delta_f H^0(298)$ and $S^0(298)$ are the standard enthalpy of formation and the standard absolute entropy, respectively, at 298.15 K. The $C_p(T)$ term is the heat capacity as a function of temperature at constant pressure. The standard enthalpy of formation and standard absolute entropy for the liquid phase pure component end-members are calculated from the solid phase values and heat of fusion, temperature of fusion, and heat capacity data: [43]

$$\Delta_f H^\circ_{liquid}(298) = \Delta_f H^\circ_{solid}(298) + \Delta H_{fus} - \int_{298}^{T_{fus}} \Delta C_{p,liquid-solid}(T)dT \qquad \textbf{3-2}$$

$$S^\circ_{liquid}(298) = S^\circ_{solid}(298) + \frac{\Delta H_{fus}}{T_{fus}} - \int_{298}^{T_{fus}} \frac{\Delta C_{p,liquid-solid}(T)}{T}\,dT \qquad \textbf{3-3}$$

The requisite experimental data may not exist for some intermediate compounds that are formed in certain solid phases of some of the binary or higher order systems. In these instances, it will be necessary to approximate the missing enthalpy of formation, absolute entropy, or heat capacity. This is often completed by optimizing these parameters in the model to provide a best fit of the

phase diagram to the experimental data points, by estimating the values as the weighted average of the end-member properties, or potentially some iterative combination of different estimation techniques. The Neumann-Kopp rule can be used when calculating the weighted average for heat capacity values [72]. These methods were utilized in estimating the values for the intermediate solid compounds in the CsF-BeF_2 and RbF-BeF_2 binary systems (e.g., $CsBeF_3$). Additionally, an empirical correlation for absolute entropy was developed for some types of molten salt compounds during the MSRP [86, 87].

3.2.2 Solid and Liquid Solutions

An example of thermodynamic information which describes the non-ideal behavior exhibited by solutions is a binary or ternary phase diagram. Such a phase diagram can be used by FactSage to find excess energy parameters which are used by the solution model to fit a calculated phase diagram to the experimental one. The phase diagrams (or corresponding excess energy parameters) which provided this information to be included in the thermodynamic database of the 9-element system are outlined in Table 3-1. In some cases, existing excess Gibbs free energy functions from the literature were modified so they could be incorporated into the model (marked as "Model modified?" in Table 3-1). Three binaries had not previously been optimized in the literature and were optimized as part of this study (marked as "Optimized in this study?" in Table 3-1).

Experimental data from the above binary and ternary systems (e.g., liquidus and solidus temperatures) can be used to calculate and optimize phase diagrams in FactSage which in turn helps solve for the Gibbs energy of the system at each temperature and composition. Gibbs free energy minimization dictates the phase distribution in the system, resulting in an estimation of the phase equilibria, i.e., if the compound is part of a solid solution, liquid solution, gas phase, or pure component. The molar Gibbs energy of the solution phases is given by the following expression:

$$G_m = G_m^{\circ} + G_m^{id} + G_m^{xs} \qquad \textbf{3-4}$$

where G_m° is the weighted molar Gibbs energy of the pure end-member solution components, G_m^{id} is an ideal Gibbs energy of mixing term (ideal configurational entropy), and G_m^{xs} is the excess Gibbs free energy (non-ideal).

Following the definition provided in equation 3-4, the equation for the total Gibbs energy of a binary solution is written as:

$$G(T) = x_1 \cdot G_{m,1}^{\circ}(T) + x_2 \cdot G_{m,2}^{\circ}(T) + x_1 RT ln x_1 + x_2 RT ln x_2 + G_m^{xs} \qquad \textbf{3-5}$$

where x_1 and x_2 are the mole fractions of end-member species 1 and 2, respectively, R is the ideal gas constant in $J \cdot mol^{-1} \cdot K^{-1}$, and T is the temperature in Kelvin. As an example, the following polynomial formalism has been used to describe the Gibbs excess energy for some simple binary systems:

$$G_m^{xs} = \sum_{ij} x_1^i \cdot x_2^j \cdot (A + BT + CT\, ln\, T + DT^2 \ldots) \qquad \textbf{3-6}$$

Table 3-1: List of binary and ternary systems included in the thermochemical model

	System components			Included in the model?	Experimental data in the literature?	Model modified?	Optimized in this study?	Reference
Binary Systems	LiF	BeF_2		✓	✓	✓	–	[88]
	LiF	CsF		✓	✓	–	–	[72]
	LiF	UF_4		✓	✓	–	–	[89]
	LiF	UF_3		✓	✓	–	✓	[55]
	BeF_2	CsF		✓	✓	–	✓	[90]
	BeF_2	UF_4		✓	✓	–	–	[91]
	BeF_2	UF_3		–	–	–	–	–
	CsF	UF_4		–	✓	–	–	[55]
	CsF	UF_3		–	–	–	–	–
	UF_4	UF_3		✓	✓	–	–	[42]
	RbF	LiF		✓	✓	✓	–	[92]
	RbF	BeF_2		✓	✓	–	✓	[55]
	RbF	UF_4		–	✓	–	–	[55]
	RbF	ZrF_4		–	✓	–	–	[55]
	RbF	CsF		✓	✓	✓	–	[93]
	ZrF_4	LiF		✓	✓	✓	–	[90]
	ZrF_4	BeF_2		✓	✓	✓	–	[90]
	ZrF_4	UF_4		✓	✓	✓	–	[90]
	ZrF_4	CsF		–	✓	–	–	[55]
	CsF	CsI		✓	✓	✓	–	[72]
	LiF	LiI		✓	✓	–	–	[72]
	LiI	CsI		✓	✓	✓	–	[72]
Ternary Systems	LiF	BeF_2	UF_4	✓	✓	–	–	[91]
	LiF	BeF_2	ZrF_4	✓	✓	✓	–	[90]
	BeF_2	ZrF_4	UF_4	–	✓	–	–	[90]
	LiF	BeF_2	RbF	–	✓	–	–	[55]
	LiF	RbF	UF_4	–	✓	–	–	[55]

where x_1^i and x_2^j are the mole fractions of end-member species 1 and 2 to the ith and jth power, respectively, and the coefficients A, B, C, and D are parameters that are fit during optimizations to experimental data. A separate solution database was created for each solid solution using the "one-lattice polynomial model" (QKTO) in FactSage. In this FactSage model, the thermochemical data for the end-member species are defined, and the excess Gibbs free energy expressions are input in terms of the end-member species' mole fractions by selecting Add Bragg Williams → GE → Simple Polynomial.

Phase diagrams can be calculated by implementing equation 3-5 in FactSage and plotting the phase diagram curves against experimental data points, optimizing the equation to match the phase lines to the experimental data. For example, one methodology includes plotting only the terms in the equation which correspond to the ideal solution, and, if necessary, sequentially adding the ideal Gibbs energy of mixing terms, the enthalpy of mixing term, and the excess entropy of mixing term (the latter two of which make up the excess Gibbs of mixing term) [43].

The modified quasichemical model in the quadruplet approximation (MQM-TSQA) described by Pelton et al. [94] has been applied to optimize the excess Gibbs free energy functions of the liquid

solutions. The MQM-TSQA accounts for first-nearest-neighbor (FNN) and second-nearest-neighbor (SNN) short-range ordering in solutions and is the recommended method for modeling molten salt solutions because it best describes their configurational entropy [95]. In the MQM-TSQA, the system of interest is considered to be made up of a series of quadruplets (sets of 4 ions) that contain two cations and two anions. If the system of interest has 2 cations (A and B) and 2 anions (X and Y), there are nine quadruplets. These quadruplets consist of 4 unary sets ($[A_2X_2]_{quad}$, $[B_2X_2]_{quad}$, $[A_2Y_2]_{quad}$, and $[B_2Y_2]_{quad}$) that represent the 4 end-members, 4 binary sets ($[ABX_2]_{quad}$, $[ABY_2]_{quad}$, $[A_2XY]_{quad}$, and $[B_2XY]_{quad}$), and 1 reciprocal set ($[ABXY]_{quad}$). Each ion within a quadruplet has a SNN coordination number. For example, the SNN coordination number of A in quadruplet A_2X_2 is denoted $Z^{A}_{A_2/X_2}$, and it represents the number of A cations neighboring a single A cation (i.e., the cation-cation coordination number). All cation-cation coordination numbers for the 9-element system of interest were set to the default value of 6, unless noted otherwise (Table 3-2). The anion-anion coordination numbers are determined by satisfying electroneutrality. For example, the anion-anion coordination number for anion X in the ABX_2 quadruplet (Z^{X}_{AB/X_2}) is defined as follows:

$$\frac{q_A}{Z^{A}_{AB/X_2}} + \frac{q_B}{Z^{B}_{AB/X_2}} = \frac{q_X}{Z^{X}_{AB/X_2}} + \frac{q_X}{Z^{X}_{AB/X_2}} \qquad \textbf{3-7}$$

where q_A, q_B, and q_X are the absolute charges of cations A and B and anion X, respectively.

Table 3-2: Non-default cation-cation coordination numbers of liquid solutions

A	B	Z^{A}_{AB}	Z^{B}_{AB}
Li^+	Be^{2+}	3	6
Li^+	Zr^{4+}	2	6
Li^+	U^{4+}	2	6
Be^{2+}	Be^{2+}	4.8	4.8
Be^{2+}	U^{4+}	3	6
Be^{2+}	Zr^{4+}	3	6

A liquid solution database incorporating the Gibbs excess energy parameters for the binary and ternary subsystems was created in FactSage using the "two-lattice modified quasichemical model revised" (SUBQ) model. In this FactSage model, two sublattices were defined: sublattice A for the cations (Li, Be, Cs, U^{3+}, U^{4+}, Rb, and Zr) and sublattice B for the anions (F and I). Next, an end-member species for every combination of cation and anion was inputted, and the thermochemical data for the 9 liquid end-member species considered were defined. Five of the fourteen liquid end-member species were modeled as ideal compounds due to a lack of binary system information (RbI, BeI_2, UI_3, UI_4, ZrI_4). Ultimately, most of them were deemed not to be in appreciable quantities or thermodynamically preferred and so the assumption was justified, although the discovery and inclusion of binary system data for any of them can only improve the accuracy of the model, especially for some of the higher importance compounds, e.g., RbI.

Under the "End-Members" category in the solution module of FactSage, there is a place on the upper right part of the window to define the cation-cation coordination number (Z("Cation")), the anion-anion coordination number (Z("Anion")), and the ratio of the FNN to the SNN ("ζ"). The cation-cation coordination number is 6 unless defined otherwise in Table 3-2. For example, for the end-member species BeF_2, the cation-cation coordination number for Be^{2+}-Be^{2+} is 4.8. The cation-cation SNN coordination numbers for non-equivalent cations (e.g., Li^+ and Be^{2+}) were

inputted into the FactSage liquid solution model as "Non-Default Quads" because they are not part of an end-member quadruplet. The anion-anion coordination number (Z("Anion")) is automatically determined in FactSage according to equation 3-7. The variable zeta ("ζ") is calculated as follows (for the A_2X_2 quadruplet):

$$\zeta_{A/X} = 2Z^{A}_{A_2/X_2} Z^{X}_{A_2/X_2} / \left(Z^{A}_{A_2/X_2} + Z^{X}_{A_2/X_2}\right) \quad \textbf{3-8}$$

where $Z^{A}_{A_2/X_2}$ and $Z^{X}_{A_2/X_2}$ are the previously defined SNN coordination numbers of A and X in the A_2X_2 quadruplet.

Table 3-3 reports the ζ value for each end-member species (i.e., each unary quadruplet in the 9-element system). The Gibbs excess energy function of the liquid solution for an AX-BX binary system is defined as the Gibbs energy change for the SNN pair-exchange reaction:

$$(A-X-A) + (B-X-B) = 2(A-X-B) \quad \Delta g_{AB/X} \quad \textbf{3-9}$$

The Gibbs energy change parameter for a binary AX-BX system ($\Delta g_{AB/X}$) can be expanded into the following polynomial:

$$\Delta g_{AB/X} = \Delta g^{0}_{AB/X} + \sum_{(i+j \geq 1)} g^{ij}_{AB/X} \chi^{i}_{AB/X} \chi^{j}_{BA/X} \quad \textbf{3-10}$$

Table 3-3: The ζ values for each end-member species

End-member species	Quadruplet	ζ
LiF	Li_2F_2	6
BeF_2	Be_2F_2	3.2
CsF	Cs_2F_2	6
UF_3	$U^{3+}{}_2F_2$	3
UF_4	$U^{4+}{}_2F_2$	2.4
ZrF_4	Zr_2F_2	2.4
RbF	Rb_2F_2	6
LiI	Li_2I_2	6
BeI_2	Be_2I_2	3.2
CsI	Cs_2I_2	6
UI_3	$U^{3+}{}_2I_2$	3
UI_4	$U^{4+}{}_2I_2$	2.4
ZrI_4	Zr_2I_2	2.4
RbI	Rb_2I_2	6

where $\Delta g^{0}_{AB/X}$ and $g^{ij}_{AB/X}$ are composition independent (but potentially temperature dependent) coefficients that are obtained by fits to experimental data. The composition dependent $\chi_{AB/X}$ term is defined as:

$$\chi_{AB/X} = \left(\frac{X_{AA}}{X_{AA} + X_{AB} + X_{BB}}\right) \quad \textbf{3-11}$$

where X_{AA}, X_{AB}, and X_{BB} are the mole fractions of the cation-cation pairs.

Gibbs energy functions for the following liquid phase binaries were included in the 9-element system:

- $LiF\text{-}BeF_2$
- LiF-CsF
- $LiF\text{-}UF_4$
- $LiF\text{-}UF_3$
- BeF_2-CsF
- $BeF_2\text{-}UF_4$
- UF_4- UF_3
- RbF-LiF
- $RbF\text{-}BeF_2$
- RbF-CsF
- ZrF_4-LiF
- $ZrF_4\text{-}BeF_2$
- $ZrF_4\text{-}UF_4$
- CsF-CsI
- LiF-LiI
- CsI-LiI

Some of the ternary subsystems required Gibbs excess energy parameters in addition to those optimized for the binary subsystems. Excess Gibbs energy functions were included for the following liquid phase ternaries: $LiF\text{-}BeF_2\text{-}UF_4$ and $LiF\text{-}BeF_2\text{-}ZrF_4$.

The excess Gibbs free energy expressions for the binary and ternary systems were input into the FactSage liquid solution model as "Interactions" by highlighting the elements in the system under "Sublattices" in the sidebar, right-clicking, and then selecting "Add Pair Fraction Expansion → GE".

Thermodynamic models for ternary subsystems were extrapolated from the binary subsystems using the Kohler and Toop methods depending on whether the system was treated as symmetric or asymmetric, respectively. System components were grouped into 2 categories–the highly ionic, monovalent fluorides and iodides LiF, RbF, CsF, LiI, RbI, and CsI (category 1) and the polyvalent fluorides and iodides BeF_2, UF_3, UF_4, ZrF_4, BeI_2, UI_3, UI_4, ZrI_4 (category 2). Component pairs within the same category were modeled as symmetric while those between categories were modeled as asymmetric. The data extrapolation models for the higher order system were assigned in the FactSage solution database under the "Ternary Interpolations" option.

And finally, due to a lack of thermodynamic information which would quantify potential non-ideal behavior of hydrogen-containing compounds, these compounds were modeled as ideal in the 9-element system. Because most of these compounds were gases under these conditions, and thus not dissolved in the fluoride salt solution, it is believed to be a good assumption. This is handled not within the solution model itself, which was described above, but rather was handled within the equilibrium solver module, Equilib.

4 Summary

A review of literature pertaining to thermodynamic modeling of molten salts and experimental research in molten salt thermochemistry is completed. Covered are the thermodynamic principles which govern vapor-liquid equilibria, the early investigations in molten salt thermochemistry during the Molten Salt Reactor Program at ORNL, followed by developments made in modeling the thermodynamic behavior of the components in salt solutions. A methodology that is commonly employed in calculating the phase diagrams of fused salt mixtures is summarized. The process is carried out with the commercial software FactSage, which provides the ability to build a thermodynamic database of the chosen pure components (main salt components + radionuclides of interest) as well as the ability to calculate phase and chemical equilibria in the system for a specific set of conditions. The main conclusions are summarized below:

- Molten salt mixtures rarely behave as ideal liquid solutions, but their behaviors tend to follow established trends and deviations from ideality can be bounded
- This non-ideal behavior is largely due to strong electrostatic interactions, as well as some contributions from van der Waals effects
- Most cations added to fluoride salt systems experience negative (i.e., stabilizing) deviations from ideality due to beneficial Coulombic interactions, largely represented by the difference in charge and radius
- Iodide (and potentially most anions) added to fluoride salt systems at high concentrations tend to experience positive (i.e., destabilizing) deviations from ideality due to less benefits from Coulombic interactions and relatively strong contributions from dispersion forces largely represented by the difference in polarizability
- Data on iodine chemistry in melts containing beryllium fluoride are minimal and the predicted behavior of iodine in the coolant salt of KP-FHR has low confidence as a result
- The difference between the energy associated with the pure components and the Gibbs energy of the ideal solution is represented by the ideal Gibbs energy of mixing, also known as the configurational entropy term
- The difference between the Gibbs energies of the ideal solution and the real solution is represented by the excess Gibbs energy of mixing
- The degree of nonideality can be quantified by the excess Gibbs energy of mixing which also varies logarithmically with the activity coefficient for that solute at that temperature, pressure, and composition
- The excess Gibbs energy (or alternatively, the activity coefficient) is a mix of two contributions: enthalpy of mixing and excess entropy of mixing
- Enthalpy of mixing has a positive correlation with Gibbs energy, while the entropy term has a negative correlation
- Enthalpy of mixing data is easier to obtain experimentally than excess entropy of mixing data, although data for both are still lacking for many salt systems
- Excess energies can be estimated with solution models developed specifically for molten salts and similar liquid structures; currently preferred is the modified quasichemical model (MQM)
- MQM relies on experimental thermodynamic data of both the pure components and the binary systems of each couple of end-members of the mixture, typically as binary phase diagrams
- A methodology for building a thermodynamic database with FactSage based on MQM and the CALPHAD method is outlined
- Speciation calculations in FactSage with the thermodynamic database can be used to estimate activity coefficients based on Raoult's law and knowledge of the pure component vapor pressures

Bibliography

[1] J. W. McMurray and T. M. Besmann, "Thermodynamic Modeling of Nuclear Fuel Materials," in *Handbook of Materials Modeling*, 2020, pp. 2335-2363.

[2] M. H. A. Piro *et al.*, "Coupled thermochemical, isotopic evolution and heat transfer simulations in highly irradiated UO2 nuclear fuel," *Journal of Nuclear Materials*, vol. 441, no. 1-3, pp. 240-251, 2013.

[3] A. L. Smith and R. J. M. Konings, "Reaction kinetics and chemical thermodynamics of nuclear materials," in *Advances in Nuclear Fuel Chemistry*, 2020, pp. 3-88.

[4] M. H. A. Piro, "Computational thermochemistry of nuclear fuel," in *Advances in Nuclear Fuel Chemistry*, 2020, pp. 159-182.

[5] S. I. Sandler, *Chemical, biochemical, and engineering thermodynamics*, 4th ed. John Wiley & Sons, 2006.

[6] W. B. White, S. M. Johnson, and G. B. Dantzig, "Chemical Equilibrium in Complex Mixtures," *The Journal of Chemical Physics*, vol. 28, no. 5, pp. 751-755, 1958.

[7] R. Privat *et al.*, "Teaching the Concept of Gibbs Energy Minimization through Its Application to Phase-Equilibrium Calculation," *Journal of Chemical Education*, vol. 93, no. 9, pp. 1569-1577, 2016.

[8] M. Blander, "Thermodynamic properties of molten salt solutions," CONF-8608157-2, 1986.

[9] "Aircraft Nuclear Propulsion Project Quarterly Progress Report for Period Ending December 31, 1956," Oak Ridge National Laboratory, ORNL-2221, 1957.

[10] "Aircraft Nuclear Propulsion Project Quarterly Progress Report for Period Ending June 30, 1957," Oak Ridge National Laboratory, ORNL-2340, 1957.

[11] "Aircraft Nuclear Propulsion Project Quarterly Progress Report for Period Ending September 10, 1956," Oak Ridge National Laboratory, ORNL-2157, 1956.

[12] "Aircraft Nuclear Propulsion Project Quarterly Progress Report for Period Ending March 31, 1957," Oak Ridge National Laboratory, ORNL-2274, 1957.

[13] "Aircraft Nuclear Propulsion Project Quarterly Progress Report for Period Ending December 31, 1957," Oak Ridge National Laboratory, ORNL-2440, 1957.

[14] "Reactor Chemistry Division Annual Progress Report for Period Ending January 31, 1963," Oak Ridge National Laboratory, ORNL-3417, 1963.

[15] S. Cantor, "Freezing Point Depressions in Sodium Fluoride. Effect of Alkaline Earth Fluorides," *The Journal of Physical Chemistry*, vol. 65, no. 12, pp. 2208-2210, 1961.

[16] "Reactor Chemistry Division Annual Progress Report for Period Ending January 31, 1962," Oak Ridge National Laboratory, ORNL-3262, 1962.

[17] "Reactor Chemistry Division Annual Progress Report for Period Ending January 31, 1961," Oak Ridge National Laboratory, ORNL-3127, 1961.

[18] M. Blander, "Van der Waals Energy Changes in the Mixing of Molten Salts," *The Journal of Chemical Physics,* vol. 36, no. 4, pp. 1092-1093, 1962.

[19] "Chemistry Division Annual Progress Report for Period Ending May 31, 1971," Oak Ridge National Laboratory, ORNL-4706, 1971.

[20] M. Blander, "Max Bredig Award Acceptance Speech: Creating a Crystal Ball for Molten Salt Solutions," presented at the ECS Meeting, Joint International Symposium on Molten Salts, Honolulu, HI, USA, October 18-23, 1987.

[21] H. Flood, T. Førland, and K. Grjotheim, "Über den Zusammenhang zwischen Konzentrationen und Aktivitäten in geschmolzenen Salzmischungen," *Zeitschrift für anorganische und allgemeine Chemie,* vol. 276, no. 5-6, pp. 289-315, 1954.

[22] M. Blander and J. Braunstein, "A quasi-lattice model of molten reciprocal salt systems," *Annals of the New York Academy of Sciences (US),* vol. 79, 1960.

[23] M. Blander, "Quasi-Lattice Model of Reciprocal Salt Systems. A Generalized Calculation," *The Journal of Chemical Physics,* vol. 34, no. 2, pp. 432-438, 1961.

[24] M. Blander and M. L. Saboungi, "The coordination cluster theory - Application to ternary reciprocal molten salt systems," *Acta Chemica Scandinavica,* vol. 34, pp. 671-676, 1980.

[25] M. L. Saboungi, D. Caveny, I. Bloom, and M. Blander, "The coordination cluster theory - Extension to multicomponent systems," *Metallurgical Transactions A,* vol. 18A, pp. 1779-1783, 1987.

[26] H. Reiss, J. L. Katz, and O. J. Kleppa, "Theory of the Heats of Mixing of Certain Fused Salts," *The Journal of Chemical Physics,* vol. 36, no. 1, pp. 144-148, 1962.

[27] M. Blander, "Excess Free Energies and Heats of Mixing in Certain Molten Salt Mixtures," *The Journal of Chemical Physics,* vol. 37, no. 1, pp. 172-173, 1962.

[28] M. Blander and S. J. Yosim, "Conformal Ionic Mixtures," *The Journal of Chemical Physics,* vol. 39, no. 10, pp. 2610-2616, 1963.

[29] M. L. Saboungi, H. Schnyders, M. S. Foster, and M. Blander, "Phase diagrams of reciprocal molten salt systems. Calculations of liquid-liquid miscibility gaps," *The Journal of Physical Chemistry,* vol. 78, no. 11, pp. 1091-1096, 1974.

[30] M. L. Saboungi and M. Blander, "Topology of Liquidus Phase Diagrams of Charge-Asymmetric Reciprocal Molten Salt Systems," *Journal of the American Ceramic Society,* vol. 58, no. 1-2, 1975.

[31] M. L. Saboungi and M. Blander, "Conformal ionic solution theory for additive ternary molten–ionic systems," *The Journal of Chemical Physics,* vol. 63, no. 1, pp. 212-220, 1975.

[32] M. L. Saboungi, "Calculation of thermodynamic properties of multicomponent ionic reciprocal systems," *The Journal of Chemical Physics,* vol. 73, no. 11, pp. 5800-5806, 1980.

[33] M. Blander and A. D. Pelton, "Thermodynamic analysis of binary liquid silicates and prediction of ternary solution properties by modified quasichemical equations," *Geochimica et Cosmochimica Acta,* vol. 51, pp. 85-95, 1987.

[34] A. D. Pelton and M. Blander, "Thermodynamic analysis of ordered liquid solutions by a modified quasichemical approach - application to silicate slags," *Metallurgical Transactions B,* vol. 17B, pp. 805-815, 1986.

[35] A. D. Pelton and M. Blander, "A least squares optimization technique for the analysis of thermooynamic data in ordered liquids," *Calphad,* vol. 12, no. 1, pp. 97-108, 1988.

[36] A. D. Pelton, S. A. Degterov, G. Eriksson, C. Robelin, and Y. Dessureault, "The modified quasichemical model - I. Binary solutions," *Metallurgical and Materials Transactions B,* vol. 31B, pp. 651-659, 2000.

[37] A. D. Pelton and P. Chartrand, "The modified quasi-chemical model: Part II. Multicomponent solutions," *Metallurgical and Materials Transactions A,* vol. 32A, pp. 1355-1360, 2001.

[38] P. Chartrand and A. D. Pelton, "The modified quasi-chemical model: Part III. Two sublattices," *Metallurgical and Materials Transactions A,* vol. 32A, pp. 1397-1407, 2001.

[39] P. Chartrand and A. D. Pelton, "Thermodynamic evaluation and optimization of the LiCl-NaCl-KCl-RbCl-CsCl-MgCl2-CaCl2 system using the modified quasi-chemical model," *Metallurgical and Materials Transactions A,* vol. 32A, pp. 1361-1383, 2001.

[40] P. Chartrand and A. D. Pelton, "Thermodynamic evaluation and optimization of the LiF-NaF-KF-MgF2-CaF2 system using the modified quasi-chemical model," *Metallurgical and Materials Transactions A,* vol. 32A, pp. 1385-1396, 2001.

[41] P. Chartrand and A. D. Pelton, "Thermodynamic evaluation and optimization of the Li, Na, K, Mg, Ca // F, Cl reciprocal system using the modified quasi-chemical model," *Metallurgical and Materials Transactions A,* vol. 32A, pp. 1417-1430, 2001.

[42] J. McMurray, T. Besmann, J. Ard, S. Utlak, and R. Lefebvre, "Status of the molten salt thermodynamic database, MSTDB," in "ORNL/SPR-2019/1208," 2019.

[43] O. Beneš and R. J. M. Konings, "Thermodynamic Calculations of Molten-Salt Reactor Fuel Systems," in *Molten Salts Chemistry - From Lab to Applications,* 2013, pp. 49-78.

[44] D. Grabaskas *et al.*, "Regulatory Technology Development Plan - SFR Mechanistic Source Term Trial Calculation," Argonne National Laboratory, ANL-ART-49, October 2016.

[45] "Molten-Salt Reactor Program Semiannual Progress Report for Period Ending February 29, 1972," Oak Ridge National Laboratory, ORNL-4782, 1972.

[46] "Molten-Salt Reactor Program Semiannual Progress Report for Period Ending February 29, 1968," Oak Ridge National Laboratory, ORNL-4254, 1968.

[47] "Molten-Salt Reactor Program Semiannual Progress Report for Period Ending August 31, 1967," Oak Ridge National Laboratory, ORNL-4191, 1967.

[48] S. T. Lam, Q.-J. Li, J. Mailoa, C. Forsberg, R. Ballinger, and J. Li, "The impact of hydrogen valence on its bonding and transport in molten fluoride salts," *Journal of Materials Chemistry A,* vol. 9, no. 3, pp. 1784-1794, 2021.

[49] "Molten-Salt Reactor Program Semiannual Progress Report for Period Ending August 31, 1972," Oak Ridge National Laboratory, ORNL-4832, 1973.

[50] A. P. Malinauskas and D. M. Richardson, "The Solubilities of Hydrogen, Deuterium, and Helium in Molten Li2BeF4," *Industrial & Engineering Chemistry Fundamentals,* vol. 13, no. 3, pp. 242-245, 1974.

[51] P. E. Field and J. H. Shaffer, "The solubilities of hydrogen fluoride and deuterium fluoride in molten fluorides," *The Journal of Physical Chemistry,* vol. 71, no. 10, pp. 3218-3222, 1967.

[52] "Reactor Chemistry Division Annual Progress Report for Period Ending December 31, 1965," Oak Ridge National Laboratory, ORNL-3913, 1966.

[53] "Molten-Salt Reactor Program Semiannual Progress Report for Period Ending August 31, 1965," Oak Ridge National Laboratory, ORNL-3872, 1965.

[54] O. N. Breusov, A. V. Novoselova, and I. P. Simanov, "Thermal and x-ray phase analyses of the system CsF-BeF2 and its relationship to systems of the type MIF-BeF2," *Doklady Akademii nauk SSSR (Proceedings of the USSR Academy of Sciences),* vol. 118, pp. 935-937, 1958.

[55] R. E. Thoma, "Phase Diagrams of Nuclear Reactor Materials," Oak Ridge National Laboratory, ORNL-2548, 1959.

[56] J. Lumsden, "Thermodynamics of molten mixtures of alkali-metal halides," *Discussions of the Faraday Society,* vol. 32, pp. 138-146, 1961.

[57] J. L. Holm and O. J. Kleppa, "Enthalpies of Mixing in Binary Liquid Alkali Fluoride Mixtures," *The Journal of Chemical Physics,* vol. 49, no. 5, pp. 2425-2430, 1968.

[58] L. S. Hersh and O. J. Kleppa, "Enthalpies of Mixing in Some Binary Liquid Halide Mixtures," *The Journal of Chemical Physics,* vol. 42, no. 4, pp. 1309-1322, 1965.

[59] O. J. Kleppa, *Thermodynamic properties of molten salt solutions* (Thermodynamics in Geology, Proceedings of the NATO Advanced Study Institute held in Oxford, England, September 17–27, 1976). Springer, Dordrecht, 1977.

[60] "Molten-Salt Reactor Program Quarterly Progress Report for Period Ending June 30, 1958," Oak Ridge National Laboratory, ORNL-2551, 1958.

[61] "Molten-Salt Reactor Program Semiannual Progress Report for Period Ending August 31, 1971," Oak Ridge National Laboratory, ORNL-4728, 1972.

[62] "Reactor Chemistry Division Annual Progress Report for Period Ending January 31, 1965," Oak Ridge National Laboratory, ORNL-3789, 1965.

[63] G. D. Robbins, R. E. Thoma, and H. Insley, "Phase equilibria in the system CsF-ZrF4," *J. Inorg. Nucl. Chem.,* vol. 27, pp. 559-568, 1965.

[64] "Reactor Chemistry Division Annual Progress Report for Period Ending December 31, 1966," Oak Ridge National Laboratory, ORNL-4076, 1967.

[65] "Molten-Salt Reactor Program Semiannual Progress Report for Period Ending January 31, 1963," Oak Ridge National Laboratory, ORNL-3419, 1963.

[66] M. E. Melnichak and O. J. Kleppa, "Enthalpies of Mixing in Binary Liquid Alkali Iodide Mixtures," *The Journal of Chemical Physics,* vol. 52, no. 4, pp. 1790-1794, 1970.

[67] Y. Sekiguchi, K. Uozumi, K. Kawamura, and T. Terai, "Thermodynamic analysis of molten alkali halide mixtures by molecular dynamic simulations," *Journal of Molecular Liquids,* vol. 315, 2020.

[68] M. E. Melnichak and O. J. Kleppa, "Enthalpies of Mixing in the Binary Liquid Systems Alk(Cl–Br), Alk(Cl–I), and Alk(Br–I)," *The Journal of Chemical Physics,* vol. 57, no. 12, pp. 5231-5241, 1972.

[69] C. Margheritis, G. Flor, and C. Sinistri, "Miscibility Gaps in Fused Salts: Note VII. Systems of LiF with Alkali Halides," *Zeitschrift für Naturforschung A,* vol. 28, no. 8, pp. 1329-1334, 1973.

[70] M. Taira, Y. Arita, and M. Yamawaki, "The Evaporation Behavior of Volatile Fission Products in FLiNaK Salt," *The Open Access Journal of Science and Technology,* vol. 5, no. 5, pp. 1-17, 2017.

[71] Y. Sekiguchi, K. Uozumi, T. Koyama, and T. Terai, "Fundamental study on the vaporization of cesium and iodine dissolved in LiF-NaF-KF molten salt," *Journal of Nuclear Materials,* vol. 522, pp. 136-143, 2019.

[72] E. Capelli, O. Beneš, and R. J. M. Konings, "Thermodynamics of soluble fission products cesium and iodine in the Molten Salt Reactor," *Journal of Nuclear Materials,* vol. 501, pp. 238-252, 2018.

[73] "Molten-Salt Reactor Program Semiannual Progress Report for Period Ending February 28, 1969," Oak Ridge National Laboratory, ORNL-4396, 1969.

[74] "Molten-Salt Reactor Program Semiannual Progress Report for Period Ending February 28, 1971," Oak Ridge National Laboratory, ORNL-4676, 1971.

[75] M. Blander, "Contributions to molten salt chemistry by Ole J. Kleppa," *Journal of Alloys and Compounds*, vol. 321, no. 2, pp. 164-168, 2001.

[76] M. Blander and L. E. Topol, "Complex ion formation and non-random mixing in molten reciprocal salt solutions," *Electrochimica Acta*, vol. 10, no. 12, pp. 1161-1168, 1965.

[77] "Molten-Salt Reactor Program Semiannual Progress Report for Period Ending August 31, 1974," Oak Ridge National Laboratory, ORNL-5011, 1975.

[78] C. F. Baes, R. P. Wichner, C. E. Bamberger, and B. F. Freasier, "Removal of Iodide from LiF-BeF2 Melts by HF-H2 Sparging—An Application to Iodine Removal from Molten Salt Breeder Reactor Fuel," *Nuclear Science and Engineering*, vol. 56, no. 4, pp. 399-410, 1975.

[79] P. J. Spencer, "A brief history of CALPHAD," *Calphad*, vol. 32, no. 1, pp. 1-8, 2008.

[80] C. W. Bale *et al.*, "FactSage Thermochemical Software and Databases - Recent Developments," *Calphad*, vol. 33, no. 2, pp. 295-311, 2009.

[81] M. H. A. Piro, S. Simunovic, and T. M. Besmann, "Thermochimica User Manual v1.0," Oak Ridge National Laboratory, ORNL/TM-2012/576, December 2012.

[82] M. H. A. Piro, S. Simunovic, T. M. Besmann, B. J. Lewis, and W. T. Thompson, "The thermochemistry library Thermochimica," *Computational Materials Science*, vol. 67, pp. 266-272, 2013.

[83] T. M. Besmann, J. C. Ard, K. E. Johnson, M. S. Christian, and J. A. Yingling, "The Molten Salt Thermodynamic Database (MSTDB): A Resource for MSR Design, Development, and Regulation," presented at the American Nuclear Society, Virtual Conference, June 8-11, 2020.

[84] J. Ard *et al.*, "FY20 Status report on the Molten Salt Thermodynamic Database (MSTDB) development," Oak Ridge National Laboratory, ORNL/SPR-2020/1648, September 2020.

[85] (2021, March 29). *NEA Thermodynamics of Advanced Fuels International Database updates*. Available: https://www.oecd-nea.org/jcms/pl_53310/nea-thermodynamics-of-advanced-fuels-international-database-updates

[86] "Molten-Salt Reactor Program Semiannual Progress Report for Period Ending August 31, 1970," Oak Ridge National Laboratory, ORNL-4622, 1971.

[87] "Reactor Chemistry Division Annual Progress Report for Period Ending May 31, 1971," Oak Ridge National Laboratory, ORNL-4717, 1971.

[88] O. Beneš and R. J. M. Konings, "Thermodynamic evaluation of the (LiF+NaF+BeF2+PuF3) system: An actinide burner fuel," *The Journal of Chemical Thermodynamics,* vol. 41, no. 10, pp. 1086-1095, 2009/10/01/ 2009.

[89] O. Beneš, M. Beilmann, and R. J. M. Konings, "Thermodynamic assessment of the LiF–NaF–ThF4–UF4 system," *Journal of Nuclear Materials,* vol. 405, no. 2, pp. 186-198, 2010/10/15/ 2010.

[90] O. Beneš and R. J. M. Konings, "Thermodynamic study of LiF–BeF2–ZrF4–UF4 system," *Journal of Alloys and Compounds,* vol. 452, no. 1, pp. 110-115, 2008.

[91] E. Capelli, O. Beneš, and R. J. M. Konings, "Thermodynamic assessment of the LiF–NaF–BeF2–ThF4–UF4 system," *Journal of Nuclear Materials,* vol. 449, no. 1, pp. 111-121, 2014/06/01/ 2014.

[92] O. Beneš, J. P. M. van der Meer, and R. J. M. Konings, "Modelling and calculation of the phase diagrams of the LiF–NaF–RbF–LaF3 system," *Calphad,* vol. 31, no. 2, pp. 209-216, 2007.

[93] O. Beneš, P. Zeller, M. Salanne, and R. J. M. Konings, "Density functional theory, molecular dynamics, and differential scanning calorimetry study of the RbF–CsF phase diagram," *The Journal of Chemical Physics,* vol. 130, no. 13, p. 134716, 2009/04/07 2009.

[94] A. D. Pelton, P. Chartrand, and G. Eriksson, "The modified quasi-chemical model: Part IV. Two-sublattice quadruplet approximation," *Metallurgical and Materials Transactions A,* vol. 32A, pp. 1409-1416, 2001.

[95] J. McMurray *et al.*, "Multi-Physics Simulations for Molten Salt Reactor Evaluation - Chemistry Modeling and Database Development," in "ORNL/SPR-2018/864," 2018.

Nuclear Science and Engineering
Argonne National Laboratory
9700 South Cass Avenue, Bldg. 208
Argonne, IL 60439

www.anl.gov

Argonne National Laboratory is a U.S. Department of Energy laboratory managed by UChicago Argonne, LLC